



**Application of modulation excitation-phase sensitive
detection-DRIFTS for in situ/operando characterization of
heterogeneous catalysts**

Journal:	<i>Reaction Chemistry & Engineering</i>
Manuscript ID	RE-ART-01-2019-000011.R1
Article Type:	Paper
Date Submitted by the Author:	03-Mar-2019
Complete List of Authors:	Srinivasan, Priya; The University of Kansas, Chemical & Petroleum Engineering Department; The University of Kansas, Center for Environmentally Beneficial Catalysis Patil, Bhagyasha; The University of Kansas, Department of Chemical & Petroleum Engineering; The University of Kansas, Center for Environmentally Beneficial Catalysis Zhu, Hongda; The University of Kansas, Center of Environmentally Beneficial Catalysis Bravo-Suárez, Juan; The University of Kansas, Chemical & Petroleum Engineering Department; The University of Kansas, Center for Environmentally Beneficial Catalysis



Journal Name

ARTICLE

Application of modulation excitation-phase sensitive detection-DRIFTS for in situ/operando characterization of heterogeneous catalysts

Received 00th January 20xx,
Accepted 00th January 20xx

DOI: 10.1039/x0xx00000x

www.rsc.org/

Priya D. Srinivasan,^{ab} Bhagyesh S. Patil,^{ab} Hongda Zhu,^b and Juan J. Bravo-Suárez^{*ab}

This work describes the application of in situ/operando modulation excitation-phase sensitive detection-diffuse reflectance Fourier transform spectroscopy (ME-PSD-DRIFTS) for characterization of heterogeneous catalysts. ME was enabled by a low void-volume diffuse reflectance cell which allowed rapid gas exchange (gas residence times < 2 s) and by periodic feed concentration changes to the reaction cell by a simple switching valve system that provided quasi-square shaped modulation. PSD analysis of a relatively large data set of rapid scan spectra over many periodic cycles was done via discrete Fourier transform (DFT)/frequency filtering/inverse discrete Fourier transform (IDFT). A general description of ME-PSD principle, mathematical framework, guidelines for planning, running, and interpreting results was provided while focusing on ME-PSD-DRIFTS. Aspects such as modulation frequency and amplitude, modulation waveform, sampling rate, in situ cell residence time, and future opportunities for ME-PSD-DRIFTS were also discussed. The proposed DFT/IDFT methodology uncovered the use of frequency magnitude plots for evaluation of spectra baseline shifts, signal response to modulation, response waveform type, noise, and signal decay/growth. Additionally, ethanol dehydration on γ -Al₂O₃ was presented as an example of application of the ME-PSD-DRIFTS methodology.

1. Introduction

A great number of environmentally and industrially relevant reactions are heterogeneously catalyzed and occur in the gas phase.¹ To develop new or improve current catalysts for these reactions, a better understanding of catalyst requirements and catalytic cycle are needed. This can be accomplished by a combination of in situ and operando spectroscopic characterization along with kinetic and computational studies.¹ Some of the most commonly available in situ spectroscopic techniques in catalysis laboratories are UV-Visible (UV-Vis), Fourier transform infrared (FTIR), and Raman spectroscopies.²⁻⁴ However, in situ FTIR is perhaps the most ubiquitous because of its moderate cost, relatively simple use, and ability to probe powder catalyst's surface for adsorbed species and active sites at reaction conditions.⁵ Such ability is crucial for identification of reaction intermediates to support reaction mechanisms; however, this is challenging in FTIR because the spectra arise from contributions of catalyst background, spectator species, noise, and reactive intermediate species which are usually present in small amounts and are difficult to disentangle.⁶ Therefore, advances in in situ and operando characterization techniques and sensitive spectroscopic methods are of great

importance for the study of not only active sites but also the intermediate species that take part in the catalytic reaction cycle.^{7, 8} However, at steady state conditions, identification of these short-lived active species and discrimination from the strong fingerprints of spectator species and catalyst support, which are not involved in the reaction, but usually present in high concentration, is quite complex making difficult to derive any information on mechanism and kinetics.^{9, 10}

Some of the current strategies to obtain selective information on surface intermediate species include transient techniques such as TAP (temporal analysis of products),^{11, 12} SSITKA (steady state isotopic transient kinetic analysis),^{13, 14} pure transient methods,¹⁵⁻¹⁷ and MES (modulation excitation spectroscopy).^{6, 10, 18} The main characteristic of these techniques is the introduction of a rapid perturbation (e.g., in temperature, pressure, concentration) in the system via pulses (TAP), step (SSITKA, pure transient methods), or periodic changes (MES). In TAP studies, stimulations are introduced into the system by perturbing one or two parameters such as pressure, temperature, concentration and flow rate with a sub millisecond time resolution to influence the species of interest and to analyze reaction intermediates.¹² In SSITKA,¹⁹⁻²¹ the catalyst operates at steady state chemical potential conditions, but at isotopic transients as introduced by a step change in concentration of one of the components isotope. Kinetic analysis of the resulting data thus provides information of reactive species pools. These techniques in combination with spectroscopic methods such as UV-Vis, FTIR, Raman, and X-ray absorption spectroscopies can be a powerful tool for

^a Department of Chemical & Petroleum Engineering, The University of Kansas, Lawrence, KS, 66045, USA

^b Center for Environmentally Beneficial Catalysis, The University of Kansas, 1501 Wakarusa Dr., LSRL C145F, Lawrence, KS, 66047, USA. E-mail: jibravo@ku.edu
Electronic Supplementary Information (ESI) available: [details of any supplementary information available should be included here]. See DOI: 10.1039/x0xx00000x

investigating the dynamically changing surface species and true reaction intermediates.^{3, 22} The likelihood that these spectroscopically detected surface species are involved in a catalytic cycle is usually studied by tracking changes of spectral signals to determine reaction rates, rate constants, or activation energies and match with expectations from online or bench scale reactor activity studies.^{13, 15, 17, 23} A more recent approach to detect surface reacting species has been the combination of in situ/operando spectroscopies and (e.g., concentration, temperature, pressure, etc) modulation excitation (ME) coupled with phase sensitive detection (PSD) analysis to enhance the spectra signal-to-noise ratio of reacting species while avoiding the presence of spectator species.^{6, 10, 18, 24}

In the application of ME-PSD methodology, a periodic concentration perturbation around a middle value is typically introduced in the reaction system. At this condition, the system operates in a quasi-steady state while allowing the monitoring of surface species from the transient changes.^{10, 18} While ME was initially employed as a frequency response technique for the determination of adsorption/desorption rates on heterogeneous catalysts^{25, 26} and later combined with in situ DRIFTS spectroscopy for characterization of heterogeneous catalysts,²⁷⁻³⁴ it was not until the early 2000's that Baurecht and Fringeli⁶ reported a numerical method to apply ME-PSD to in situ infrared spectroscopy. Since then, a similar ME-PSD methodology has been combined and extended to ATR,³⁵ PM-IRRAS,²⁴ DRIFTS,³⁶⁻³⁹ Raman,⁴⁰ and X-ray absorption spectroscopies⁴¹ and X-ray diffraction.^{40, 42} The original PSD methodology directly transforms in situ ME-IR spectra perturbed sinusoidally from the time-domain into the phase domain with only signals that responded to the modulation frequency.⁶ Urakawa, Bürgi, and Baiker later extended the methodology to squared waveform perturbations.²⁴

While ME-PSD, as implemented via Baurecht and Fringeli's methodology,⁶ has proved to be a major advance in the development of sensitive techniques for detection of surface reacting species in heterogeneous catalysis,^{10, 18} it is not yet widely available and has been only confined to a handful of research groups worldwide.¹⁸ One of the reasons for this is perhaps the apparent complexity of the numerical method and the cumbersome software code implementation to analyze large data sets.¹⁸ Inspired by Baurecht and Fringeli,⁶ we will report here a relatively simpler development of PSD also based on Fourier analysis, but following a procedure that is more familiar and widely available in engineering and which is not limited to a specific modulation waveform. This ME-PSD methodology is schematically shown in **Fig. 1** for in situ DRIFTS spectroscopy. Briefly, this PSD method uses Fourier transform (FT) to convert data from the time domain to the frequency domain, filters frequency or frequencies of interest (e.g., avoiding those of spectators), and recovers the filtered data via inverse Fourier transform (IFT) (into the so-called phase domain). This approach is well-known in the analysis of weak signals in the presence of a large noise as applied to mechanics (e.g., vibration analysis, nuclear power plant modelling), sonic and acoustics (e.g., passive sonar, music synthesis), biomedical engineering (e.g., cardiac patients diagnosis, ECG data

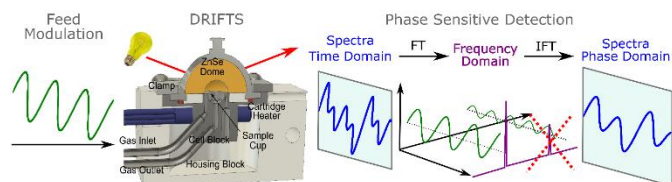


Fig. 1. General schematic representation of modulation excitation-phase sensitive detection-diffuse reflectance infrared Fourier transform spectroscopy (ME-PSD-DRIFTS) methodology.

compression), signal processing (e.g., real-time spectra analysis, speech synthesis and recognition), and instrumentation (e.g., microscopy, spectroscopy), among others.⁴³⁻⁴⁶ For practical problems requiring FT, the most common method of solution involves the discrete Fourier transform (DFT) algorithm using complex numbers. The most popular algorithm is the fast Fourier transform (FFT), which is widely available for most modern programming languages and benchmarked.⁴⁷

In this work, the application of in situ/operando ME-PSD-DRIFTS via DFT (discrete Fourier transform)/IDFT (inverse discrete Fourier transform) for characterization of heterogeneous catalysts is discussed. The principle and mathematical framework used in ME-PSD is also described. Moreover, general guidelines for planning, running, and interpreting results from ME-PSD-DRIFTS are provided including aspects such as modulation frequency and amplitude, modulation waveform, sampling rate, and in situ cell residence time. Further, ethanol dehydration on $\gamma\text{-Al}_2\text{O}_3$ is used as an example of the application of Fourier transform/inverse Fourier transform for PSD analysis of DRIFTS spectra submitted to feed concentration modulation methodology. Finally, an outlook on future opportunities to further develop the ME-PSD-DRIFTS methodology is presented. We hope this work will assist the catalysis community to better understand the application of Fourier analysis for implementation of in situ/operando ME-PSD techniques for studying reaction intermediates and active sites in heterogeneous catalysis.

2. Experimental

2.1. Reaction setup

As shown in **Fig. 1**, the experimental setup is in principle relatively simple and similar to most heterogeneous catalysts in situ spectroscopic characterization systems. It is made of a feed system that allows control of the flow rates such that a periodic concentration signal can be sent to the in situ reaction cell where surface species are monitored online. Unlike typical in situ or operando setups, there are some special requirements for feed modulation, in situ reaction cell, and spectra sampling, which will be discussed in the following sections. Regarding the feed modulation, one of the simplest systems to introduce a periodic signal is that composed of a four-way valve where two feeds are switched periodically as shown in **Fig. 2**. In the case of the in situ cell (and transfer lines), it is preferable that the void volume is minimized, mainly to allow rapid exchange of gases in the cell and to facilitate data analysis as gas concentration within the cell will tend to follow that of the input concentration. Also, the infrared spectrometer should be

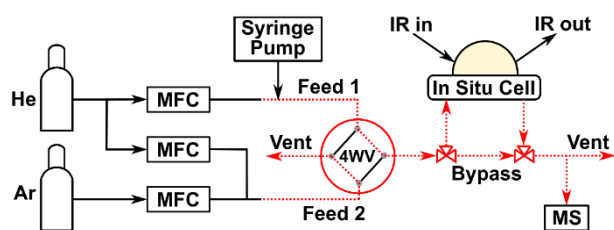


Fig. 2. Schematics of the in situ experimental setup for ME-DRIFTS. MFC = mass flow controller; MS = mass spectrometer; IR = infrared beam; 4WV = 4-port two-position (dotted and solid lines) switching valve. Dotted lines and red color indicate that transfer lines are heated to avoid possible condensation of liquid injected via the syringe pump. Adapted from Ref. 48.

capable of collecting spectra rapidly (e.g., rapid scan). Additionally, an online mass spectrometer is usually available to facilitate the rapid monitoring of gas phase products for operando studies.

For the in situ DRIFTS application described in this work (e.g., ethanol dehydration on a commercial γ - Al_2O_3 (SBa-200)), a detailed description of the reaction setup is available elsewhere, including the details (blueprints) of the design and operation of a new low-void volume in situ diffuse reflectance cell.⁴⁸ Briefly, mass flow controllers (Omega) were used to deliver and control gases flow rates to feed lines. Gas feed lines were periodically switched with a six-way switching valve (VICI) instead of a 4WV to (optionally) allow in situ cell's gas residence time distribution studies.⁴⁹ The new in situ cell resembles Harrick Scientific's HVC high reaction chamber (except it has a void volume of $\sim 1.2 \text{ cm}^3$) so that it can fit Harrick's mirror optics (Praying MantisTM). The cell possesses a monolithic ZnSe dome window (which is a special Harrick's fabrication part) that has a bottom small semi-sphere (1 cm ID) providing minimum void volume ($\sim 0.5 \text{ cm}^3$) above the sample cup. Sample temperature in the cell was monitored by a thermocouple that is in direct contact with the sample. Infrared data was acquired with an FTIR spectrometer (Vector 70, Bruker) equipped with a mercury-cadmium-telluride detector (MCT D316/BP) and with rapid scan capabilities. The outlet gases were analyzed via an online mass spectrometer (Pfeiffer, OmniStar GSD 320 O, MS).

2.2. Modulation experiment

As an example of the application of the modulation excitation-phase sensitive detection-diffuse reflectance infrared Fourier transform spectroscopy (ME-PSD-DRIFTS) methodology, ethanol conversion in the vapor phase on a commercial γ - Al_2O_3 will be described. In a typical experiment, about 45 mg of a calcined (static air, 623 K, 5 K/min, 2 h) γ - Al_2O_3 (SBa-200, Sasol, BET area = $189 \text{ m}^2/\text{g}$) catalyst (38-75 μm) were loaded to the cell. The catalyst was then heated in He (45 NTP cm^3/min , Feed 2) to 473 K. For the modulation experiment, Feed 1 (see Fig. 2) consisted of $\sim 1 \text{ kPa}$ ethanol, which was introduced via a syringe pump (60 $\mu\text{L}/\text{h}$ of liquid ethanol at ambient temperature) and carried by 40 NTP cm^3/min of He for a total flow rate of $\sim 40.4 \text{ NTP cm}^3/\text{min}$. Feed 2 was composed of a mixture of Ar/He = (10.4 NTP cm^3/min)/(30 NTP cm^3/min), where Ar was used as internal standard for mass spectrometry. Feed concentration modulation was started by switching

periodically between Feed 2 and Feed 1 flows every 45 s (via a LabVIEW 2018 VI program routine) to yield a period of 90 s ($f = 1/90 = 0.011 \text{ Hz}$). This frequency falls within the range of typical reaction TOFs for the reaction at this condition. A total of 15 periods were repeated. IR spectra were also collected simultaneously via rapid scan, about every 1 s (16 scans, 4 cm^{-1}) which matched the average gas residence in the reaction cell ($\sim 1 \text{ s}$).⁴⁸ Diffuse reflectance spectra are plotted as pseudo-absorbance, $\log(1/R)$, where R is the relative reflectance. For simplicity, they will be just noted as absorbance.⁵⁰ More details on the catalyst, reactivity, and in situ DRIFTS characterization have been recently reported.^{48, 51}

3. Modulation excitation-phase sensitive detection (ME-PSD) methodology

In a typical infrared spectrum many peaks are usually present that arise from contributions due to background, baseline shift, noise, and surface (e.g., spectator, intermediate) species that are often difficult to discriminate. Detecting intermediate species thus becomes an even more complex task as the intensity of these species tends to be small. This problem resembles the analysis of small signals in the presence of a large noise via a phase sensitive detection (PSD) method with a lock-in amplifier which makes use of Fourier transforms (FT).^{52, 53} Thus, application of FT to periodic changes of in situ infrared spectra of heterogeneous catalysts is expected to enhance the signal of intermediate species.

In the application of ME-PSD to in situ DRIFTS, the main interest is to extract with high sensitivity spectral information of surface reacting species. More specifically, one would like to detect species that could be involved in elementary steps. Here, the ME-PSD methodology employs a two-step approach. First, it introduces an external periodic perturbation to the catalyst surface (modulation excitation), which could be modulation of feed concentration, temperature, pressure, among others^{54, 55} and second, it proceeds to perform data analysis on the spectra of the perturbed catalyst surface to track only species that respond to the system modulation (phase sensitive detection).⁶ This periodic change on the catalyst surface is what enables the application of Fourier transform analysis on the modulated spectroscopic data. In general, the ME in DRIFTS is most often performed via feed concentration modulation,¹⁸ which can be done without sophisticated controls by simply switching between two flows of different gas phase concentrations or by computer programmed (e.g., Labview) periodic changes of feed gases concentration via control of flow rates with mass flow controllers. Once in situ DRIFTS data is collected over the ME experiment, the data is processed via PSD to extract information on species that respond to the frequency of feed modulation. The PSD method requires application of FT to time domain data of a periodic function resulting in a new set of data in the frequency domain. Once in the frequency domain, a filter is applied to restrict signals, usually, to the frequency of modulation, and then an inverse FT is applied to obtain the reconstructed spectroscopic data (in what is called the phase

domain) with only the species that respond to the feed modulation frequency.

3.1. Fourier analysis

In FT analysis, a periodic function $f(t)$ that varies with time and with some period T can be expressed, with little restrictions, as a Fourier series expansion in terms of an infinite sum of sines and cosines:^{6, 45, 56}

$$f(t) = \frac{1}{2}a_0 + \sum_{k=1}^{\infty} [a_k \cos(k\omega_0 t) + b_k \sin(k\omega_0 t)] \quad (1)$$

Where the angular frequency is: $\omega_0 = 2\pi/T = 2\pi f_0$, f_0 is the fundamental frequency, k is a positive integer ($k=1$ for the fundamental frequency and $k > 1$ for higher frequency harmonics), a_0 , a_k , and b_k are known as Fourier coefficients. In **eqn (1)**, the first term $a_0/2$ represents the average value of $f(t)$ over the period T . It is also interpreted as the DC term (i.e., static component of the signal) arising from contributions of species that do not respond to modulation and represented by a frequency equal to 0. The a_k and b_k are the amplitudes of the cosine (real part) and sine (imaginary part) components with angular frequency $k\omega_0$ needed to form the signal $f(t)$, respectively. Additionally, the set of a_k - and b_k -coefficients in **eqn (1)** are called the real, $\text{Re}[f(t)]$, and imaginary, $\text{Im}[f(t)]$, parts, respectively, whereas the set of all a_k - and b_k -coefficients is called the Fourier transform of $f(t)$, denoted here as $\mathcal{F}(f)$. In analogy with a polynomial equation: $p(t) = a_0 + \sum_{n=1}^N a_n t^n$ that is fitted to N points in the x - t Cartesian coordinates, the set of a -coefficients could be now called the “polynomial transform of x ”. Thus, the Fourier transform could be simply viewed as a curve fitting of a signal by a series of cosines (real part in the complex FT) and sines (imaginary part in the complex FT) and whose a_k and b_k coefficients are given by:^{6, 56, 57}

$$a_0 = \frac{2}{T} \int_{-T/2}^{T/2} f(t) dt \quad (2)$$

$$a_k = \frac{2}{T} \int_{-T/2}^{T/2} f(t) \cos(k\omega_0 t) dt; \quad k \geq 1 \quad (3)$$

$$b_k = \frac{2}{T} \int_{-T/2}^{T/2} f(t) \sin(k\omega_0 t) dt; \quad k \geq 1 \quad (4)$$

There are other convenient ways of writing the Fourier series, for example, in polar coordinates, by writing $a_k = r_k \cos(\phi_k)$ and $b_k = r_k \sin(\phi_k)$ so that **eqn (1)** becomes:

$$f(t) = \frac{1}{2}a_0 + \sum_{k=1}^{\infty} r_k \sin(k\omega_0 t + \phi_k) \quad (5)$$

Where r_k and ϕ_k are the amplitude and phase angle of the k^{th} harmonic, respectively. Here, a single sinusoid replaces each sine and cosine, and the amplitude and phase replace the previous a_k and b_k as the quantities that define the harmonics.⁵⁸ The amplitude, r_k , is proportional to the square root of the amplitude of the oscillation, whereas $|r_k|^2$ is a measure of the power contained in each harmonic. The phase angle, ϕ_k , can be useful to compare two waves. They are said to be “in-phase” when both waves’ crest are in sync or “out-of-

phase” if they have a phase difference of 180° .⁵⁸ These quantities will become more apparent in ME-PSD-DRIFTS when studying the kinetic response of various surface species responding to a modulation frequency. The amplitudes a_k and phase angles (or phase shift or phase lag or argument) ϕ_k are given by **eqns (6)** and **(7)**, respectively:^{6, 57}

$$r_k = \sqrt{(a_k^2 + b_k^2)} \quad (6)$$

$$\phi_k = \tan^{-1}\left(\frac{b_k}{a_k}\right) = \tan^{-1}\left(\frac{\text{Imaginary part}}{\text{Real part}}\right) \quad (7)$$

Despite the trigonometric and polar representation of the Fourier series, the complex exponentials is perhaps the most common way of representing the series expansion because it is easier to manipulate algebraically. By using Euler’s equation: $e^{ik\omega_0 t} = \cos k\omega_0 t + i \sin k\omega_0 t$ and the definition: $c_k = a_k/2 + b_k/2$, **eqn (1)** can then be expressed as:⁵⁶

$$f(t) = \sum_{k=-\infty}^{\infty} c_k e^{ik\omega_0 t} \quad (8)$$

Where the c_k coefficients are given by:

$$c_k = \frac{2}{T} \int_{-T/2}^{T/2} f(t) e^{-ik\omega_0 t} dt \quad (9)$$

3.2. Fourier and discrete Fourier transforms

The Fourier series (e.g., **eqn (8)**) can be used to analyze periodic functions with a period of T and a fundamental frequency of $f_0 = 1/T = \omega_0/2\pi$. A more general Fourier series, which can be also employed for analysis of non-periodic functions, is obtained from **eqns (8)** and **(9)** by letting the period to tend to infinity and the fundamental frequency to zero:^{45, 56}

$$f(t) = \int_{-\infty}^{\infty} \left[\frac{1}{2\pi} \int_{-\infty}^{\infty} f(t') e^{-i\omega t'} dt' \right] e^{i\omega t} d\omega \quad (10)$$

$$f(t) = \int_{-\infty}^{\infty} F(\omega) e^{i\omega t} d\omega \quad (11)$$

$$F(\omega) = \frac{1}{2\pi} \int_{-\infty}^{\infty} f(t) e^{-i\omega t} dt \quad (12)$$

The coefficient function $F(\omega)$ is known as the Fourier transform (FT) of $f(t)$. Thus, **eqn (12)** is employed to transform the function $f(t)$ in the time domain to the corresponding function $F(\omega)$ in the frequency domain, it is also called the analysis equation. On the other hand, **eqn (11)** is used to recover $f(t)$ from $F(\omega)$ and it is known as inverse Fourier transform (IFT) or the synthesis equation.⁵⁶ Together, the analysis (**eqn (12)**) and synthesis (**eqn (11)**) equations form what is known as the Fourier transform pair.^{45, 56, 57}

When dealing with in situ infrared spectra, data is collected as a finite series of discrete points whose explicit FT is unknown. In this case, FT is computed numerically for which **eqn (12)** integral term is approximated by finite sums. A FT calculated in this manner is called a discrete Fourier transform (DFT). For a finite-duration discrete-time signal f_m with a total of N samples, the discrete Fourier transform (DFT) and inverse discrete Fourier transform (IDFT) pair equations are given by:^{46, 57}

$$F_n = \frac{1}{N} \sum_{m=0}^{N-1} f_m e^{-i\frac{2\pi}{N}mn} \quad (13)$$

$$f_m = \sum_{k=0}^{N-1} F_k e^{i\frac{2\pi}{N}km} \quad (14)$$

Where,

$F_n = n^{\text{th}}$ DFT output component (i.e., $F_0, F_1, F_2, \dots, F_{N-1}$)

$n =$ DFT output index in the frequency domain ($n = 0, 1, 2, \dots, N - 1$)

$f_m =$ sequence of input samples (i.e., $f_0, f_1, f_2, \dots, f_{N-1}$)

$m =$ time-domain index of input samples ($m = 0, 1, 2, \dots, N - 1$)

$i = \sqrt{-1}$, and

$N =$ number of samples in the input sequence and number of frequency points in the DFT output

In eqn (13), the Fourier component $\text{Re}(F_0) = \sum f_m$ captures the static (DC) component of the signal ($\text{Im}(F_0)$ is assumed to be zero), whereas the coefficients F_n are the DFT or frequency domain representation of the discrete time signal.⁵⁷ The DFT equation described above converts in a straight manner a time-domain sequence into the corresponding frequency domain, but it is inefficient. However, an algorithm called the fast Fourier transform (FFT) developed in the 1960's significantly reduced the computational time to solve the DFT equation and is now widely available and has been implemented in many popular programming languages.^{44, 59}

3.3. DFT method

In the application of ME-PSD-DRIFTS, we used the exponential representation of the DFT as it is the standard adopted for FFT libraries. It is worth mentioning that the definitions of DFT and IDFT may differ in various references and libraries (e.g., various possibilities of assigning summation factors and exponential negative sign). These conventions should be carefully examined when applying various FFT libraries. Without loss of generality, the discussion hereinafter adopts eqn (13) as the DFT definition. The most commonly available programming languages already have available libraries or packages with handy functions for application of the phase sensitive detection methodology, that is for FT, selection of frequency or frequencies range, and IFT via the FFT algorithm, namely, `fft`, `ifft`, `fftshift`, and `ifftshift`. The last two functions sort the frequencies from minimum to maximum values. This facilitates the application of a filter to select a frequency or frequency range for IDFT in the analysis of MES data. In general, programming languages with FFT and matrix support will reduce the code length for the necessary manipulations. The use of an appropriate software language is quite convenient as it will reduce programming time to solve the DFT and IDFT equations by simply applying existing functions (e.g., `fft`, `ifft`) rather than by writing cumbersome homemade code to solve equations numerically as implied with previously reported approaches.^{6, 10, 18} In this work, we applied the `numpy`, `matplotlib`, and `wxPython` libraries for Python in a homemade program to analyze in situ DRIFTS data obtained from concentration modulated experiments.

4. MES-PSD-DRS key considerations

Fig. 3 shows a general set of decisions, not necessarily in the order presented, that need to be made before running a ME experiment including:

- What modulation frequency and amplitude should be applied?
- What modulation waveform should be used?
- What variable should be modulated?
- What is the minimum spectra sampling rate?
- Does the cell void volume matter? If so, what is the minimum residence time that should be used?

To answer these questions, currently, there is not a general set of rules to follow. Here, we will summarize some basic guidelines based on prior advances in this area for similar type of ME-ATR and ME-DRIFTS experiments^{10, 18} and their similarity with well-known periodic^{55, 60} and relaxation kinetic methods^{61, 62} for the study of chemical reactions. As in the study of periodic or frequency response methods, modulation excitation can be performed via pressure, temperature, and concentration perturbations;⁶¹ however, our focus here, for simplicity, is on concentration modulation strategies.^{60, 63, 64} This, however, does not preclude the use of pressure, temperature, or other previously reported approaches as the data collection and analysis will still be similar to those described here.^{55, 60, 61, 64}

At first look, it is difficult to realize that all questions and steps in Fig. 3 are interrelated.⁶¹ For example, it will be shown in the following sections that ultimately the experimental variables need to be chosen such that quality and amount of the collected data is sufficient to draw qualitative (e.g., presence of possible intermediate species and their interrelationship) and quantitative (e.g., elementary reaction rate constants) information from the studied system as constrained by the sensitivity and noise level of the available analytical equipment.^{61, 65} For frequency response experiments, for example, the following observations have been reported that need to be taken into account for a measurable (chemical relaxation) effect:

- Frequency.* If the oscillation frequency is much larger than the reciprocal of the (chemical) relaxation time, the amplitude of the response is zero and the system remains at steady state.⁶¹
- Frequency.* Experimental frequencies should be selected such that their inverse values are within the

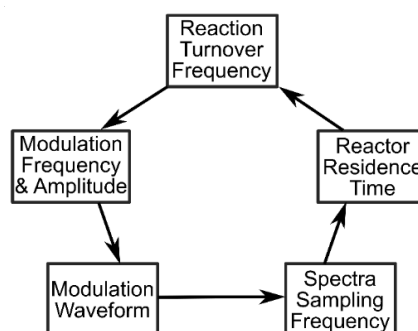


Fig. 3. General considerations in a modulation excitation spectroscopy experiment

range of the characteristic (chemical) relaxation times (for fast and slow processes) of the system under study (e.g., $0.1 \leq \omega\tau \leq 10$, where ω and τ are the modulation frequency and relaxation time of the system, respectively).^{55, 60, 61, 66, 67}

- c) *Amplitude*. The amplitude of the input perturbation is usually kept small to simplify quantitative kinetic data analysis (often <5–20%, but dependent on system).^{55, 61, 64} However, under specific circumstances (e.g., reactions can be expressed as first order or pseudo first order processes) it is possible to employ larger perturbations which result in higher precision of the measurements because of the larger observed concentration changes.⁶¹
- d) *Sampling*. Data needs to be acquired rapidly to collect a sufficient number of points per period (>50).⁵⁵
- e) *Sampling*. Amplitude changes and phase lags need to be collected over several (>5–10) steady-state cycles.^{6, 10, 55}
- f) *Analytical equipment*. Analysis methods must detect accurately phase lags (<0.1%) and amplitude attenuations (~1% of total amplitude change), specially at low and high frequencies when phase lags are small.⁵⁵
- g) *Reactor*. System volume should minimize hydrodynamic delays and allow modulation frequencies >0.01 Hz.⁵⁵
- h) *Reactor*. In mixed reactors, cycling periods are usually around 60 s (~0.017 Hz).⁶⁰

4.1. TOF vs modulation frequency and amplitude

One of the decisions to plan a ME-PSD-DRIFTS experiment requires the selection of the type of modulation and its frequency and amplitude. Although a modulation in a reactive system could be imposed by perturbations to reaction temperature, pressure, feed composition, and others,^{55, 61, 63, 65} our work and that of others on ME-PSD spectroscopic techniques over the past 16 years have focused on feed composition modulation because of the flexibility and better control on the perturbation.^{6, 10, 18, 66} The answer to what magnitude of the frequency and amplitude of the modulation should be used, however, is not a trivial one. Chemical intuition would suggest, for example, that modulation frequency should be at least of the same order of magnitude of the reaction turnover frequency and this is indeed in agreement with requirements for relaxation methods, in part because too low or too high frequencies may result in responses that are too weak or that produce minimum phase lags which preclude kinetic analysis of the data.^{55, 60, 61, 66} It is worth noting that even if significant differences exist between the reaction TOF and the modulation frequency, it may still be possible to obtain qualitative information on the detected species. While TOFs are known to vary over a wide range, for example, 10^{-6} to 10^0 s⁻¹,⁶⁸ it may be possible to modify the reaction conditions such as temperature and pressure to match TOFs with feasible modulation frequencies in the in situ reaction cell and with the available analytical equipment. For example, cycling

frequencies in mixed reactors have been reported to be in the order of 10^{-2} Hz,⁶⁰ which would place limits on the possible modulation frequencies available for testing in in situ cells. Moreover, the decision of the modulation frequency is also dependent on the sensitivity and time resolution of the analytical equipment such that a good spectral response signal-to-noise ratio can be obtained. In turn, spectra quality depends on data sampling requirements. Also, it is possible that higher frequency harmonics may be available in a single experiment depending on the modulation waveform used. This can further extend the range of frequencies at hand for evaluating surface species responses. For example, it is expected that by controlling the modulation to specific waveforms (e.g., square,²⁴ triangular, sawtooth) higher frequency harmonics will result that could be used to discern short lived (fast reacting) species.⁹ All these variables, modulation waveform, sampling frequency, and the effect of mixing (i.e., residence time) in a ME-PSD experiment will be discussed in the following sections.

Similar to the requirements for modulation frequency, the size of the perturbation change for the amplitude of the selected variable (e.g., a given reactant concentration in the feed) should be high enough that it results in measurable responses, but not too high as to oversaturate the catalyst surface or to introduce gas phase signals that could mask surface species (e.g., in ME-PSD-DRIFTS). Also, the response quality, in turn, will depend on the sensitivity and time resolution of the analytical equipment. Changes as high as 100% in the modulation amplitude with respect to an average (concentration) value have been reported for ME-PSD-DRIFTS or frequency response methods.^{27, 28, 31, 38, 48} However, changes in the order of 5–20%, which will be dependent on the system under study, have been estimated to be required to linearize rate equations (via the assumption of *small perturbations*) which simplify kinetic models to determine chemical relaxation times (related to reaction rate constants).^{55, 61} Examples of development of kinetic models to frequency response (feed concentration modulation) experiments applied to heterogeneous catalysis have been reported by the groups of Renken,²⁸ Wokaun,^{31–34} and Gonzalez.²⁷

4.2. Waveform vs frequency harmonics

The most common waveforms described in concentration ME-PSD experiments are the sine^{6, 10, 31} and square^{9, 24, 66} waveforms. The main reason for the use of the sine waveform is because of a simpler mathematic analysis of the FT equations allowing more manageable numerical methods implementation,^{6, 10, 24} however, at the expense of a more sophisticated computer controlled feed delivery system for precise control of concentration in a sine periodic fashion. The opposite is true for a square waveform, a slightly more complicated mathematical solution of the FT equations, but which can be generated with a simpler feed control system by switching between two feeds of different concentrations. As described above, the use of a square waveform has the additional advantage of generating higher frequency harmonics which could be used for inquiring the response of faster reacting

surface species.⁹ While introducing a sine or square perturbation in the feed to an in situ cell does not warrant that the response of surface species will be of the same form, it should introduce a periodicity on the surface species and active sites enabling FT type analysis as that required in the PSD methodology. Therefore, regardless of the obtained periodic form on the surface and active site species, those species that respond to the modulation frequency will be more likely to be involved in reaction elementary steps.

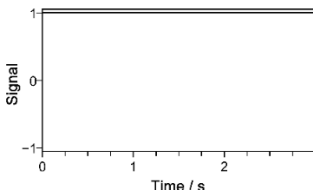
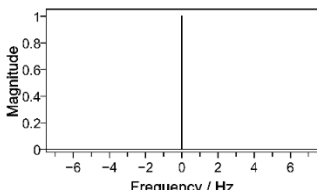
In previous reported ME-PSD approaches, very little attention was given to the resulting frequency domain of the response, which is expected to contain additional information of the response waveform, spectra baseline shifts, noise, signal decay, among others. **Table 1**, for example, presents some common nonperiodic signals and periodic waveforms and their corresponding time and frequency domain DFT-pairs. These pairs will help later in the interpretation of ME-PSD frequency domain data. For example, during feed ME-PSD only species that respond to the feed modulation frequency are more likely to be intermediate species. On the other hand, species that do not respond, namely, spectator species, and spectra background will show up in a frequency domain magnitude plot, but with a frequency of zero (Entry 1). Therefore, in the application of the IDFT with a frequency or frequencies larger than the (fundamental) modulation frequency, contributions due to spectators and background are excluded.

Entry 2 in **Table 1** indicates that noise, except that which may be periodic and with frequency higher or lower than the modulation frequency, will contribute to some extent to the reconstructed IDFT spectra. Entry 3 could be interpreted, for example, as a linear shift in the spectra baseline, and which could be assessed from the broadening around the zero frequency. Entries 4 and 5 correspond to sine or cosine waveforms showing that the corresponding frequency domain magnitude plot results in a single frequency (e.g., the modulation frequency), whereas that for the square waveform in Entry 6 shows the presence not only of the fundamental frequency, but also higher frequency harmonics. This frequency domain magnitude plot clearly shows the advantage of using a square waveform as higher frequency harmonics will be present (equivalent to single sine waveform experiments of $2k-1$ modulation frequency) and which could be employed to

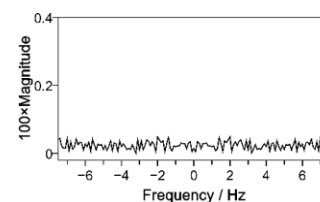
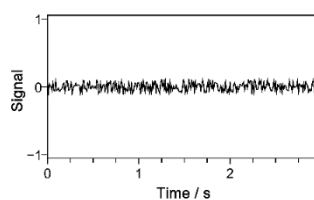
evaluate faster reacting surface species,^{9, 24} but at the expense of a response in the phase domain of lower signal-to-noise ratio quality. In general, depending on the chemical response (e.g., relaxation time) of surface species, their resulting waveform could be slightly different from that of a sine or square and possibly more likely resembling a triangle or sawtooth like waveform. In that case, higher $2k-1$ and k harmonics may be expected as shown from Entries 7 and 8, respectively.

In summary, regardless of the modulation waveform, the frequency domain magnitude plot of the spectral response can provide additional information to assess the quality of the collected data such as the presence of baseline shifts and deviations from the modulation waveform, but more importantly if selected species respond to the perturbation, in which case, the observed fundamental frequency (i.e., the most intense) should match the modulation frequency. Also, application of DFT/IDFT via commonly available FFT algorithms (implemented in widely available software packages) further facilitate the use of almost any type of periodic modulation form and its corresponding analysis, further increasing our ability to extract more information of surface species that respond to periodic perturbations and their possible relevance in elementary steps of catalytic cycles. For example, based on Entry 9, and in analogy with NMR spectroscopy, a decaying sine waveform will result in a broad fundamental frequency similar to that observed in free induction decay (FID) signal and its corresponding frequency domain. Thus, we anticipate that, at least in principle, from a decaying response waveform it is possible to determine the relative kinetic response (e.g., relaxation time) of different species from the broadening of the fundamental frequency in a frequency domain magnitude plot. This is particularly interesting as kinetic information of surface species could be obtained in a single experiment with a decaying waveform with a single frequency and not in multiple experiments with varying modulation frequencies as it has been usually performed.^{27, 31-34} Another consequence of the presence of a decaying waveform (not introduced deliberately as a feed modulation) is that ME-PSD could in theory be also expanded to the study of deactivating catalysts. This is a broadly unexplored area where we expect ME-PSD techniques to make further contributions to the understanding of active sites and intermediate species in heterogeneous catalysis.

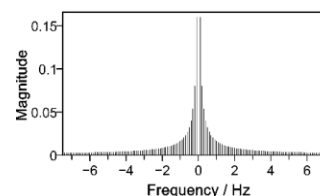
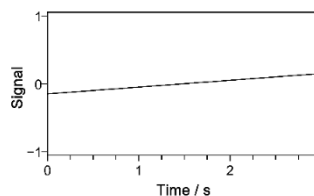
Table 1. Common nonperiodic signals and periodic waveforms, time domain, and their frequency domain magnitude^{44,67}

Nonperiodic signals and periodic waveforms	Time domain signal	Frequency domain - magnitude
1: Constant ($f(t) \equiv 1$)		

2: Noise (random)



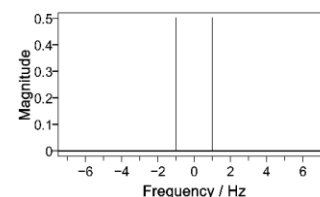
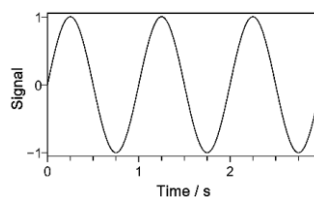
3: Linear



4: Sine (amplitude=1, period=1)

$$f(t) = \sin(\omega_0 t)$$

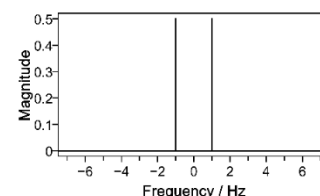
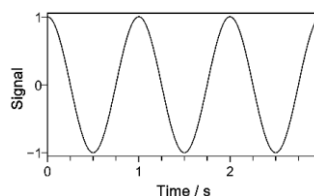
$$= \frac{1}{2i} [\exp(i\omega_0 t) - \exp(-i\omega_0 t)]$$



5: Cosine (amplitude=1, period=1)

$$f(t) = \cos(\omega_0 t)$$

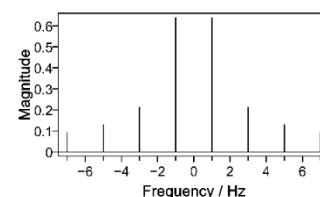
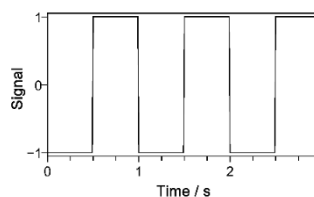
$$= \frac{1}{2} [\exp(i\omega_0 t) + \exp(-i\omega_0 t)]$$



6: Square (amplitude=1, period=1)

$$f(t) = \frac{4}{\pi} \sum_{k=1}^{\infty} \frac{\sin[(2k-1)\omega_0 t]}{2k-1}$$

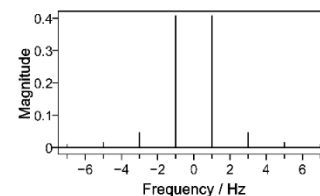
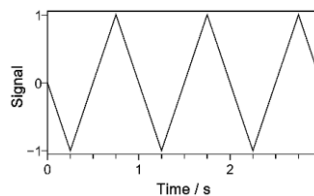
$$= \frac{2}{\pi i} \sum_{k=-\infty}^{\infty} \frac{\exp[i(2k-1)\omega_0 t]}{2k-1}$$



7: Triangular (amplitude=1, period=1)

$$f(t) = \frac{8}{\pi^2} \sum_{k=1}^{\infty} \frac{(-1)^{k+1} \sin[(2k-1)\omega_0 t]}{(2k-1)^2}$$

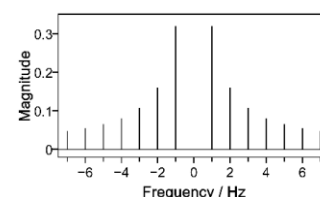
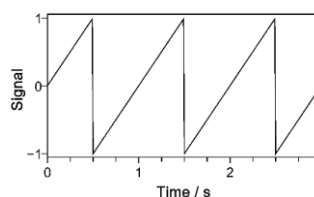
$$= \frac{4}{\pi^2 i} \sum_{k=-\infty}^{\infty} \frac{(-1)^{k+1} \exp[i(2k-1)\omega_0 t]}{(2k-1)^2}$$



8: Sawtooth (amplitude=1, period=1)

$$f(t) = \frac{2}{\pi} \sum_{k=1}^{\infty} \frac{(-1)^{k+1} \sin(k\omega_0 t)}{k}$$

$$= \frac{1}{\pi i} \sum_{k=-\infty, k \neq 0}^{\infty} \frac{(-1)^{k+1} \exp(ik\omega_0 t)}{k}$$

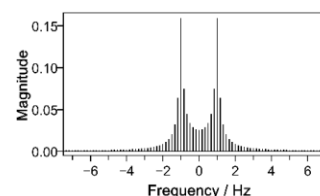
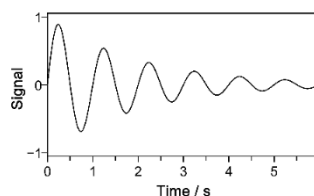


9: Decaying sine (initial amplitude=1, period=1,

decay constant=0.5 s⁻¹)

$$f(t) = e^{-k_d t} \sin(\omega_0 t)$$

$$= \frac{e^{-k_d t}}{2i} [\exp(i\omega_0 t) - \exp(-i\omega_0 t)]$$



4.3. Minimum sampling rate

An additional question to ask in planning ME-PSD experiments is how fast should data be collected? While the

obvious answer would be as fast as possible with the available analytical equipment, this is not satisfactory because of the nature of the sampling of a continuous signal. To answer this

question, we refer to the theory of signal processing and more specifically to the Nyquist-Shannon sampling theorem that states that proper sampling of a continuous function requires a sampling frequency that is at least twice that of the highest frequency in the signal.⁶⁹ When such condition is met, the original signal form can be recreated from the sampled data via Fourier analysis, otherwise the reconstructed signal form will be different from the original where high frequencies appear as artifacts at low frequencies in the sampled signal (aliasing).⁴⁶ In a ME-PSD-DRIFTS experiment, for example, when employing a sine waveform, one would reasonably expect the response to follow the fundamental modulation frequency (Table 1, Entry 4). Therefore, at the very least a sampling frequency of $2f_0$ would suffice. In the case of a square waveform, because of the presence of higher harmonic frequencies (Table 1, Entry 6), the highest frequency of the response signal is unknown, but often it will likely not exceed $9f_0$. Therefore, in such a case, $18f_0$ could be used as a safe minimum sampling frequency.

4.4. Reaction cell residence time

Another aspect that requires careful consideration is the fluid dynamic characteristics of the in situ reaction cell employed in the ME-PSD-DRIFTS experiments. It is expected that diffuse reflectance (DR) reaction cells with minimum void volume ($<1-2\text{ cm}^3$), as encountered in bench scale fixed bed reactors or in transmission reaction cells,² will be favorable for ME-PSD experiments as gas exchange within the cell should be rapid (i.e., low residence time) following concentration changes due to feed perturbation introduced in the reaction system. Such stringent low void volume requirements for in situ DR cells bring experimental complications as low void volume cells ($<1-2\text{ cm}^3$) are not currently commercially available² and those which have been reported in the literature are not easily reproducible.⁷⁰⁻⁷³ Despite these limitations, ME-PSD-DRIFTS experiments have been reported in the literature with commercial cells (e.g., Spectra-Tech,^{32, 74} Specac,^{31, 34, 75} Pike,^{29, 38} Harrick^{36, 37, 76-80}). Based on the design specifications of these cells,² and our recent study of mean residence time distribution in a modified Harrick DR cell,⁴⁹ it is very unlikely that any of these reaction cells is able to achieve rapid exchange of feed gases within a couple of seconds or less at reasonable gas flow rates ($<100\text{ cm}^3\text{ min}^{-1}$, to avoid pressure drop through the cell). For this reason, we recently reported the design (including the blueprints) of a new low void-volume ($\sim 1.0\text{ cm}^3$) DR reaction cell, that is relatively easy to reproduce in most catalysis laboratories with machining capabilities, and that exhibited an average gas residence time in the cell of $\sim 1.3\text{ s}$ at a total gas flow rate of $45\text{ cm}^3/\text{min}$.⁴⁸ If ME-PSD-DRIFTS experiments have been reported with large void volume reaction cells, then, a question to ask would be: is a low void volume cell required for these experiments? or in other words, what is the average residence time required for ME-PSD-DRIFTS?

An obvious answer to the above question would be the lowest residence time possible. However, as discussed in previous sections, there is not a simple answer because of the interrelationship between gas residence time and feed

modulation frequency and amplitude to yield a good spectral response with the time resolution limitations of the available analytical equipment (e.g., rapid scan FTIR, mass spectrometer). For frequency response techniques, for example, previous authors have reported that void volume should be minimized to obtain frequencies above 0.01 Hz ,⁵⁵ which appears to be the case for mixed reactors where cycling periods of around 60 s ($\sim 0.017\text{ Hz}$) are achievable.⁶⁰ If we follow previous suggestions of at least 50 data points (i.e., spectra) per period or the minimum number of samples based on a square waveform (assuming conservatively that the highest frequency is $\sim 10f_0 \approx 0.017\text{ Hz}$),⁵⁵ then at least a sampling frequency of 0.35 Hz (0.35 samples/s) would be needed or the equivalent of 1 spectra every 3 s. This sampling frequency ($1-3\text{ spectra/s}$) is readily achievable in most current FTIR spectrometers with rapid scan capabilities at a reasonable resolution. Therefore, a time of $<1-3\text{ s}$ would probably be a good first guess for the average residence time in the reaction cell to match the time resolution of the spectrometer.

It can be argued that large void volume cells can yield similar results as those of low void volume ones. In analogy with the system behavior to different modulation frequencies, intuitively one would expect this to be true. For example, in low void volume cells the gas phase modulation frequency and concentration amplitude within the cell should match closely that expected from the input waveform because of the rapid gas exchange. In a larger void volume cell, the gas phase concentration frequency will still match that of the waveform, thus allowing ME-PSD analysis. However, the gas phase concentration amplitude should be attenuated because of the slower gas phase exchange within the cell.⁴⁸ Therefore, large void volume cells could be used for ME-PSD-DRIFTS experiments, but because of attenuation the system response could likely have a lower signal-to-noise ratio under the experimental reaction conditions. To match the performance of a low void volume cell, larger concentration amplitude changes would be needed, which carry the risk of introducing significant gas phase contributions in the resulting spectra. Overall, this suggests that large void volume cells will require more careful preliminary tests to ensure proper performance and the absence of gas phase contributions. In order to better explore the interrelation between cell void volume (i.e., residence time) and modulation frequency and amplitude, the next section explores the in situ cell gas phase concentration and the recorded outlet concentration in a mass spectrometer as modelled by a two CSTR reactors in series. Such model roughly represents the reaction cell setup shown in Fig. 2 as demonstrated in recent reports for a homemade low void-volume⁴⁸ and large void-volume commercial Harrick cell.⁴⁹

4.4.1. Feed modulation and in situ reaction cell frequency response model. In the study of residence time distribution for the in situ reaction cell shown in Fig. 2, it has been shown that the cell and the MS analysis chamber can be approximated as continuously stirred tank reactors in series.^{48, 49} We are interested in investigating the output concentration behavior from the in situ cell as a function of the cell average residence

time and modulation frequency for a given modulation waveform. This is a classical type of problem used in process control to study the response to a disturbance in a continuously stirred tank reactor (its solution is available in many textbooks), for example, to attenuate concentration changes in an upstream process stream before delivery to a downstream plant.⁸¹ Below, a solution of the problem is presented based on Fourier series with a fundamental angular frequency $\omega_0 = 2\pi f_0$, bounded by $[-1, 1]$, and for a square waveform (Table 1, Entry 6).

For a square waveform, the input signal is given by:

$$f(t) = \frac{4}{\pi} \sum_{k=1}^{\infty} \frac{\sin[(2k-1)\omega_0 t]}{2k-1} = \frac{2}{\pi i} \sum_{k=-\infty}^{\infty} \frac{\exp[i(2k-1)\omega_0 t]}{2k-1} \quad (15)$$

Thus, after solution of the two CSTR model the following Fourier series express the outputs from the CSTR1 (in situ cell) and CSTR2 (MS) after the modulation is steady.

$$f_1(t) = \frac{2}{\pi i} \sum_{k=-\infty}^{\infty} \frac{\exp[i(2k-1)\omega_0 t]}{(2k-1)[1+i(2k-1)\omega_0\tau_1]} \quad (16)$$

$$f_2(t) = \frac{2}{\pi i} \sum_{k=-\infty}^{\infty} \frac{\exp[i(2k-1)\omega_0 t]}{(2k-1)[1+i(2k-1)\omega_0\tau_1][1+i(2k-1)\omega_0\tau_2]} \quad (17)$$

A detailed derivation, description of the equations, and the solutions for other waveform types are provided as supporting material (Section S1, Table S1, Figs. S1-S2). Eqns (16) and (17) are then used to predict the output concentrations of the in situ cell (CSTR1) and MS (CSTR2) characterized by average residence times τ_1 and τ_2 , respectively, which are forced to a square input modulation of angular frequency ω_0 as given by eqn (15). Based on the in situ cell characteristics described above, a $\tau_1=1$ s is used to characterize a low void-volume cell⁴⁸ and a $\tau_1=25$ s is used to describe a relatively large void-volume cell at moderate gas flow rates (~ 45 cm³/min).⁴⁹

Fig. 4 shows the residence time distribution in a typical low void-volume ($\tau_1 = 1$ s) in situ cell subjected to a square waveform input signal of frequencies $f_0 = 0.011$, 0.033, and 0.10 Hz and an amplitude of 0.5. The conditions of Fig. 4A are typical of ME-PSD-DRIFTS experiments.⁴⁸ The results show that the

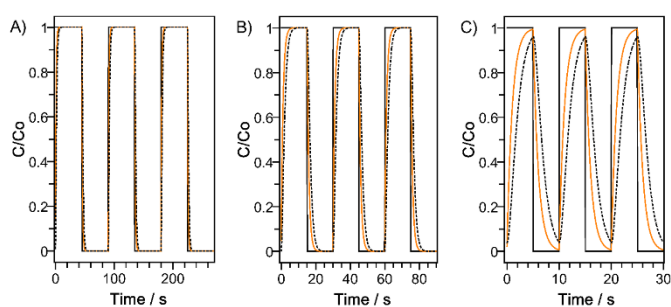


Fig. 4. Residence time distribution simulation of two CSTR reactors in series (in absence of reaction) by inducing a square waveform with a periodic concentration change in the feed with periods of: A) 90 s ($f_0 = 0.011$ Hz), B) 30 s ($f_0 = 0.033$ Hz), and C) 10 s ($f_0 = 0.1$ Hz). First reactor simulates a low void-volume reaction cell and the second simulates the mass spectrometer mixing chamber. Concentration exiting CSTR #1 = orange, solid line; concentration exiting CSTR #2 = black, dotted line. Conditions: (CSTR #1 average residence time) $\tau_1 = 1$ s; (CSTR #2 average residence time) $\tau_2 = 1$ s; (feed modulation low relative concentration) $C_{low}/C_0 = 0$; (feed modulation low relative concentration) $C_{high}/C_0 = 1$.

concentration within the cell (solid orange line) tracks closely with the input waveform (solid black line) at the f_0 between 0.011 and 0.033 Hz. Only when $f_0 = 0.10$ Hz is used, the feed concentration in the cell (i.e., same as the CSTR1 output in absence of reaction) takes more of a triangular shape (with slightly reduced amplitude) despite the use of square waveform as the input. This result highlights the interrelation between modulation frequency and amplitude and mixing in the reaction cell. Clearly, for a cell with a residence time = 1 s (e.g., low void-volume), concentration attenuation (slight change in amplitude) only becomes significant after an almost tenfold increase in the modulation frequency in the 0.01–0.1 Hz range, but with a distortion in the response modulation waveform. It is worth noticing that these results only account for the effect of mixing within the cell; however, it is likely that the waveform shape may be more accentuated once adsorption and reaction (i.e., chemical relaxation time) are also taken into account. If the sought concentration amplitude changes within the cell with respect to a central value are based on the changes from the input signal, then the results here illustrate that preliminary testing is not necessary for typical modulation frequencies (e.g., 0.01–0.1 Hz) in a low void-volume cell as the concentration changes tracked with those expected from the input modulation. Additionally, if mixing within the MS analysis chamber was minimum at the studied modulation frequency, then one would expect output concentrations CSTR1 (solid orange line) and CSTR2 (dashed black line) to be only slightly delayed as observed for Figs. 4A and 4B. These results also highlight possible risks of analyzing phase shifts based on MS data without taking into account the effect of mixing within the MS analysis chamber at relatively high modulation frequencies.^{48, 49}

Fig. 5 shows the residence time distribution in a relatively large void-volume ($\tau_1 = 25$ s) in situ cell subjected to a square waveform input signal of frequencies $f_0 = 0.011$, 0.033, and 0.10 Hz and an amplitude of 0.5.⁴⁹ Unlike the results in Fig. 4 for a low void-volume cell, these results indicate that, as expected, a larger void-volume can significantly attenuate the cell feed concentration. At comparable conditions, a larger void-volume at 0.011 Hz (Fig. 5A) will have a large concentration amplitude

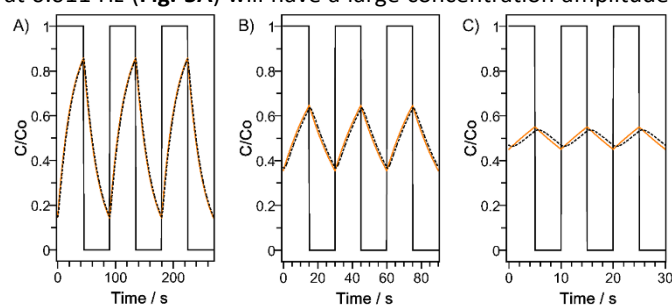


Fig. 5. Residence time distribution simulation of two CSTR reactors in series (in absence of reaction) by inducing a square waveform with a periodic concentration change in the feed with periods of: A) 90 s ($f_0 = 0.011$ Hz), B) 30 s ($f_0 = 0.033$ Hz), and C) 10 s ($f_0 = 0.1$ Hz). First reactor simulates a large void-volume reaction cell and the second simulates the mass spectrometer mixing chamber. Concentration exiting CSTR #1 = orange, solid line; concentration exiting CSTR #2 = black, dotted line. Conditions: (CSTR #1 average residence time) $\tau_1 = 25$ s; (CSTR #2 average residence time) $\tau_2 = 1$ s; (feed modulation low relative concentration) $C_{low}/C_0 = 0$; (feed modulation low relative concentration) $C_{high}/C_0 = 1$.

variation, despite the relatively lower modulation frequency. Further increases in modulation frequencies will simply continue to attenuate the output signal such that only about 10% of the original amplitude will be noticeable at a modulation frequency of 0.10 Hz. Such dramatic concentration amplitude changes within the cell make it more difficult to plan ME-PSD-DRIFTS experiments in absence of a mixing description of the reaction cell used. Also, if the analytical equipment is unable to capture the smaller amplitude changes of the response (e.g., spectra, output concentrations) within the cell, then higher input concentrations will be required. This presents additional experimental issues as gas phase contributions may be more prominent and could affect the resulting phase domain spectra results.

In summary, significant attenuation of the response waveform (i.e., concentration amplitude), with respect to that of the input modulation within the cell, was observed at relatively high enough modulation frequencies and at large cell residence times such as those usually found at typical flow conditions (e.g., 45 cm³/min) in large void-volume (e.g., 13 cm³) commercial reaction cells.⁴⁹ Such effects are minimized when using low void-volume cells (~1 cm³) in which lower residence times (~1 s) are more easily achievable.⁴⁸ Another advantage of low void-volume cells is that amplitude changes within the cell are expected to track more closely with those expected from the input periodic perturbation, which greatly facilitates the planning of ME-PSD-DRIFTS experiments and further quantitative analysis of the results.

5. ME-PSD-DRIFTS application example: ethanol dehydration on γ -Al₂O₃

Ethanol dehydration on γ -Al₂O₃ was selected as an example to demonstrate the application of ME-PSD-DRIFTS.⁵¹ On γ -Al₂O₃, ethanol conversion to diethyl ether at low temperatures has been hypothesized to occur via an S_N2 mechanism in which adsorbed ethanol and an incipient ethoxide species react to produce diethyl ether and water.^{82, 83} Additionally, ethanol conversion to ethylene is usually favored at higher temperatures via an E2 mechanism with adsorbed ethanol as intermediate species.^{82, 83} Also, the active sites are believed to be strong Lewis acid-weak Brønsted base pair sites present on several facets of Al₂O₃.^{82, 84-91} Here, the conversion of ethanol at 473 K and total pressure of 101.3 kPa is reported. At these conditions, the main product of reaction was diethyl ether (5.9 mmol/g_{cat}/h) and ethylene to a lesser extent (0.2 mmol/g_{cat}/h) as determined in a fixed bed reactor (473 K, 1 kPa EtOH, total gas flow rate ≈ 80 cm³/min, catalyst weight = 76 mg). Additional catalyst characterization, reactivity and kinetic tests were communicated recently,⁵¹ but here the focus is on the application of ME-PSD-DRIFTS as discussed below. Fig. 6 shows possible reaction intermediates in the conversion of ethanol to ethylene and diethyl ether which may be detected via in situ ME-PSD-DRIFTS as described in the following sections.

5.1. Time domain spectra

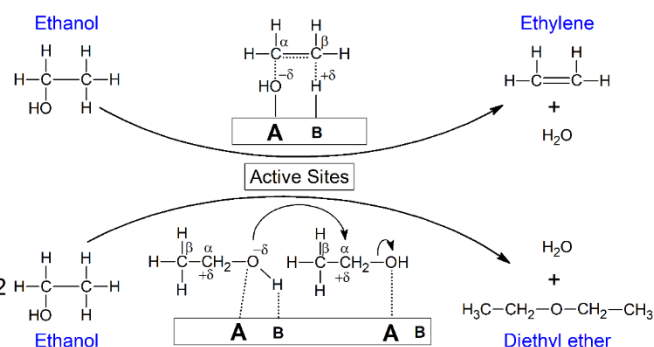


Fig. 6. Ethanol conversion to ethylene and diethyl ether via E2 (adsorbed ethanol intermediate) and S_N2 (incipient ethoxide species and adsorbed ethanol intermediates) mechanisms, respectively.

Fig. 7 shows the in situ time domain ME-DRIFTS spectra during ethanol dehydration on γ -Al₂O₃ at 473 K as ethanol concentration rises to a maximum within the reaction cell during the first 45 s (0–45 s: He/EtOH (1 kPa) and 45–90 s: Ar/He) of the 12th ME periodic cycle. Small changes can be seen as ethanol concentration increases, however, these are not obvious as spectra is dominated by strong sample background and peaks that do not change significantly during the modulation. The peaks identified in Fig. 7 correspond closely to some of those that will be shown to respond to the feed modulation (e.g., 3730, 3674, 3230, 2975, 2929, 2873, 1445, and 1385 cm⁻¹) and some that did not change significantly (e.g., ~1700–1500 cm⁻¹). Also, the spectra showed low signal-to-noise in the region below 1200 cm⁻¹, that will also persist to some extent in the frequency and phase domains (Figs. S3-S5).

5.2. Fourier transform (FT): time domain, MS response, and frequency domain results

The in situ ME-DRIFTS results in Fig. 8A show the evolution of ethanol derived adsorbed species as tracked by the C–H stretching signal at 2967 cm⁻¹. The results indicate that it took approximately 4 cycles to reach a quasi-steady state. In typical ME-PSD-DRIFTS experiments, these first 4 cycles would be usually discarded and only the last 11 be used for PSD analysis. As implied from Section 4, there is no need to discard this data

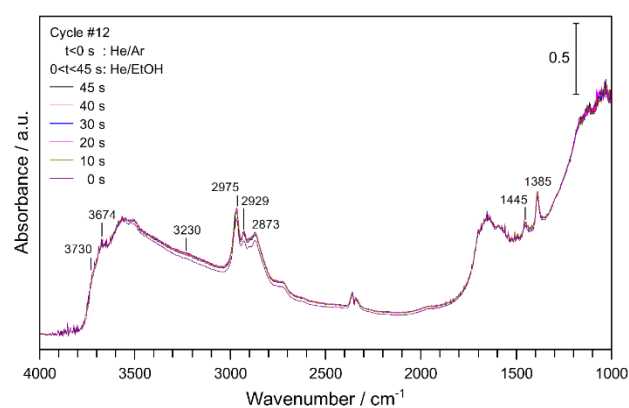


Fig. 7. In situ time domain of ME-PSD-DRIFTS during ethanol conversion on γ -Al₂O₃. Conditions: 473 K, 101.3 kPa, feed modulation from He/Ar → He + EtOH (1 kPa), modulation frequency = 1/90 Hz, total gas flow ~45 NTP cm³/min, catalyst weight ~45 mg.

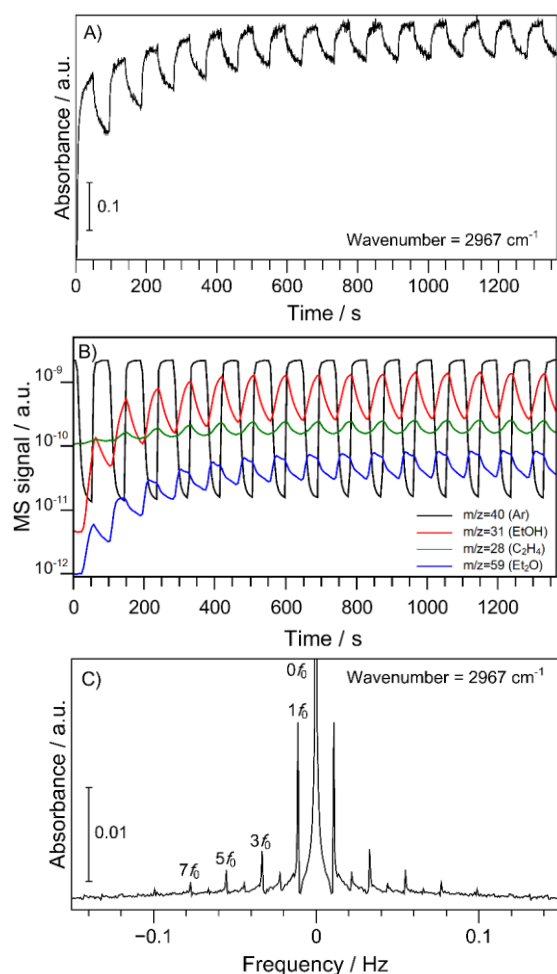


Fig. 8. In situ ME-PSD-DRIFTS during ethanol conversion on γ - Al_2O_3 . A) Time domain response plot for peak at wavenumber = 2967 cm^{-1} ; B) MS signal response plot of cell outlet gases; C) Frequency domain magnitude plot for peak at wavenumber = 2967 cm^{-1} . Conditions: 473 K, 101.3 kPa, feed modulation from He/Ar \rightarrow He + EtOH (1 kPa), modulation frequency = $1/90\text{ Hz}$, total gas flow $\sim 45\text{ NTP cm}^3/\text{min}$, catalyst weight $\sim 45\text{ mg}$.

when performing PSD via DFT + frequency filtering + IDFT process. When kept, these subtle spectral changes (small decrease in amplitude and baseline shift) in the time domain data will be reflected in the obtained frequency domain magnitude plot as broad frequency peaks (at $k=0$ for background, and $k=1, 2, 3, \dots$, for fundamental and higher frequency harmonics), for example, as shown for linear shifts and periodic decaying (or growth) of signals (Table 1, Entries 3 and 9).

Fig. 8B presents the MS signals due to the outlet gases from the in situ cell as ethanol reacted on γ - Al_2O_3 during the periodic changes from He/Ar to EtOH/He gas environments. The ethylene ($m/z=28$) and diethyl ether ($m/z=59$) gas phase concentration changes tracked with the adsorbed surface species and ethanol ($m/z=31$) outlet concentration, indicating that ethylene and diethyl ether formed from ethanol, that their formation is dependent on ethanol partial pressure, and that ethanol adsorbed reversibly on the catalyst surface. The results of the internal standard (Ar) and of cycles bypassing the cell (not shown) indicated that the input signal is dominated by a quasi-square waveform, which is similar to that observed for the

ethanol adsorbed species (Fig. 8A). Such response form indicates that the corresponding expected frequency domain magnitude plot should have peaks mostly due to the fundamental frequency and $2k-1$ higher frequency harmonics.

Fig. 8C shows the frequency domain magnitude plot for the peak corresponding to wavenumber = 2967 cm^{-1} from the in situ ME-DRIFTS during ethanol conversion on γ - Al_2O_3 . In agreement with expectations from the results of Figs. 8A and 8B and the discussion above, the frequency domain magnitude plot (Fig. 8C) is mainly constituted by the main frequency peaks of $1f_0$, $3f_0$, $5f_0$, and $7f_0$ (f_0 = feed modulation frequency) as the square waveform dominates the C–H stretching response (Fig. 8A). The presence of even ($2k$) higher frequency harmonics indicates that the response is not a perfect square waveform and that it is somewhat distorted with likely contributions of a sawtooth waveform (Table 1, Entry 8). In general, the observation of fundamental and higher harmonic frequencies in Fig. 8C confirmed that the species defined by the peak at 2967 cm^{-1} responded to the feed concentration modulation change and it is possibly an intermediate species during ethanol conversion. A discussion of the implications of the presence of higher harmonics is presented in Section 5.3. Additionally, the broad frequency peak at $0f_0$ confirmed the presence of a constant background signal, spectator species (which do not respond to feed modulation), and a shifting baseline as shown in Fig. 8A (Table 1, Entries 1 and 3). Moreover, the slight broadening of the fundamental and higher harmonic frequencies indicates a moderate decay/growth of the signal (Table 1, Entry 9) as also observed from Fig. 8A.

To summarize:

- 1) The feed modulation of 0.011 Hz used in the ME-PSD-DRIFTS experiments was within the same order of magnitude of typical TOFs for ethanol dehydration at moderate temperatures.⁵¹
- 2) The amplitude change of the feed modulation was about 60% of a middle ethanol concentration of $\sim 0.45\text{ kPa}$, which is relatively large but sufficient to produce a measurable response of the surface species as shown later. This amplitude change is in line with previous ME-DRIFTS works that reported changes of around 50–100%.^{27, 28, 31, 38, 48} At these conditions, it is possible to carry out kinetic analysis of intermediate species as previously reported by Renken,²⁸ Wokaun,³¹⁻³⁴ and Gonzalez.²⁷ For kinetic analysis such as in the determination of reaction rate constants, it is also possible to apply chemical relaxation techniques, for which it is more convenient to employ modulation amplitude changes within 5–20%.^{61, 65} At these relatively small periodic concentration changes, rate equations can be simplified by linearization allowing the direct determination of chemical relaxation times and their relationship to reaction rate constants.^{61, 65} In the present work, no attempt was made to carry out kinetic analysis of the data, but it is a current topic of research in our group.
- 3) The results in Fig. 8 indicated that a feed modulation of 0.011 Hz results in response frequencies as high as $\sim 0.08\text{ Hz}$ ($7f_0$). This corresponds to a sampling frequency of 0.16 Hz or 6.3 samples/s in concordance with Shannon-Nyquist

minimum sampling requirement. Because the rapid scan measurements reported here allowed sampling of ~ 1 spectra/s, our data sampling surpass the minimum required and can be rigorously used for PSD analysis via the DFT+IDFT methodology.

5.3. Inverse Fourier transform (IFT) results

In the previous section, it was shown that the DFT of the ME-DRIFTS data results, among other information, in the determination of frequency domain magnitude plots (Fig. 8C) which allow a critical assessment of the quality of the data and the spectral response to the feed modulation. This step was omitted in prior applications of ME-PSD.^{10, 18, 24} It was shown above that such plot is rich in information about spectra background, modulation and response waveforms, decaying/growing spectral signal trends, and signal response to modulation. In prior reports of ME-PSD methodology, the focus was on the resulting phase domain and phase shift of spectral signals, in other words, the IDFT of the FT spectral data after restricting the response only to that of signals responding to the frequency of modulation. With the information shown so far, the phase domain plots as well as phase angle (argument) plots at a given modulation frequency can be determined. In the example of Fig. 8C, it is clear that the data can be filtered at the fundamental frequency ($1f_0$) or higher frequency harmonics ($3f_0$, $5f_0$, $7f_0$) allowing the study of slow and faster reacting surface species and/or the changes in surface coverages. Ferri and co-workers,²⁴ for example, reported ME-PSD-DRIFTS during 5%NO/He \leftrightarrow 5%CO/He modulation (period = 132 s) to monitor Rh structural changes on Rh/Al₂O₃ at 573 K. The obtained phase domain spectra at $1f_0$ and $5f_0$ evidenced the presence of surface species of different kinetic behaviour. The intensity of the species with slower kinetics (CO_L, CO_B = linearly and bridge bonded CO on metallic Rh) was found to attenuate more than that of the species with faster kinetics (Al-NCO = isocyanate species coordinated to octahedral and tetrahedral sites on the Al₂O₃ support) at the higher $5f_0$ harmonic. Recently, this behavior was demonstrated mathematically by these authors by comparison of the predicted phase angular dependence for two species with different reaction rate constants while varying the response frequencies from $1f_0$ to $9f_0$.⁹ Such response is also analogous to that shown in Figs. 4 and 5, where higher modulation frequencies attenuate more significantly the concentration of species with slower kinetics (i.e., slow exchange, Fig. 5) than that of species with faster kinetics (i.e., fast exchange, Fig. 4).

5.3.1. IFT frequency filtering results. Fig. 9 presents the in situ ME-PSD-DRIFTS phase domain spectra at different response frequencies of ethanol conversion on γ -Al₂O₃. Fig. 9A, for example, shows the phase domain spectra for frequencies in the $0f_0$ – $1f_0$ (0–0.011 Hz) range for the maximum C–H stretching at a cycle time of 35 s (140° phase angle). The spectra is similar to the time domain spectra shown in Fig. 7, as expected, since the $0f_0$ captures all signals in the spectra that do not respond to feed modulation (e.g., baseline, background, spectators, etc),

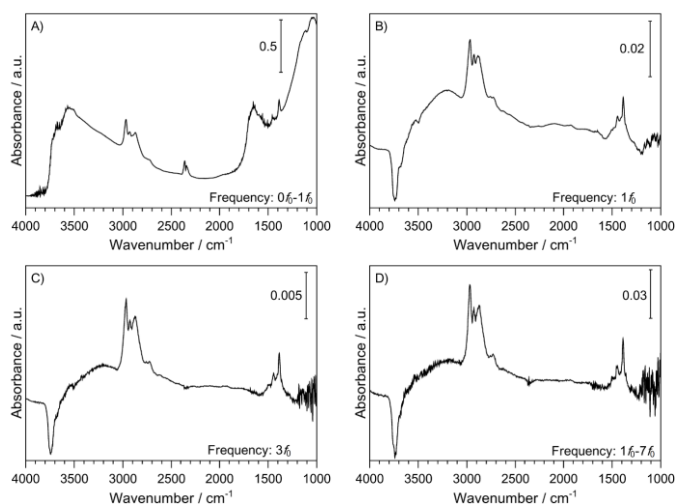


Fig. 9. In situ ME-PSD-DRIFTS phase domain spectra during ethanol conversion on γ -Al₂O₃. A) frequency response: $0f_0$ – $1f_0$ (at maximum C–H stretching cycle time, 35 s); B) frequency response: $1f_0$ (at maximum C–H stretching cycle time, 35 s); C) frequency response: $3f_0$ (at maximum C–H stretching cycle time, ~ 16 s); D) frequency response: $1f_0$ – $7f_0$ (at maximum C–H stretching cycle time, 35 s). Conditions: 473 K, 101.3 kPa, feed modulation from He/Ar \rightarrow He + EtOH (1 kPa), modulation frequency = 1/90 Hz (period = 90 s), total gas flow ~ 45 NTP cm³/min, catalyst weight ~ 45 mg. Phase angle = (time in s/period in s) $\times 360^\circ$.

whereas, the $1f_0$ response frequency captures species responding to the periodic perturbation at a modulation frequency of $1f_0$. Essentially, the original spectrum was reproduced to a great extent by including $0f_0$ in the range of frequencies for IDFT. While no new information was gained in this process, it is important from a pedagogic point of view to illustrate the PSD methodology and its ability to restrict IDFT of the ME data to a selected range of frequencies.

Fig. 9B shows more clearly the effect of frequency selection for IDFT. In this figure, the phase domain spectrum has been restricted to only the fundamental frequency, $1f_0$ (i.e., 0.011 Hz). Here, the phase domain spectrum reflects only the species that respond to the fundamental frequency and which are more likely to be intermediate species in ethanol conversion on γ -Al₂O₃ at 473 K. While the absorbance intensity is significantly smaller in Fig. 9B than the original time domain spectrum (Fig. 7 or Fig. 9A), it does highlight the power of the PSD methodology as various peaks are now discernible which were not easily observed in the time domain spectrum (Fig. 9A). Assignment of these peaks will be made in more detail in the following section as here the focus is to highlight the selection of different modulation frequencies for phase domain (i.e., IDFT) spectra reconstruction.

Fig. 9C shows the phase domain spectrum for maximum C–H stretching signal during ethanol conversion on γ -Al₂O₃ at 473 K and as limited to the higher frequency harmonic $3f_0$ (i.e., 0.033 Hz). It has been recently reported that the ME-PSD analysis at frequencies higher than the fundamental one allows discrimination of faster reacting reaction species.⁹ Comparison of Figs. 9B and 9C indicates that both spectra are almost identical, except with a slight decrease in the intensity of broad peaks around 3300–3200 cm⁻¹ and an increase in the noise of the signal below 1200 cm⁻¹. Such differences suggest the existence of species in the 3300–3200 cm⁻¹ that adsorb or react

at different rates² and of a decrease in the signal-to-noise ratio as a result of the smaller intensity of the $3f_0$ response frequency.²⁴ A further increase in the response frequencies from $1f_0$ – $7f_0$ for IDFT spectra reconstruction resulted in a similar spectrum with no significant gain in new information. Therefore, for this example, phase domain spectra reconstruction at the fundamental frequency captures all species that respond to the feed modulation.

It should be stressed here that the observed relationship between ethanol and reaction products (in the gas phase, **Fig. 8**) and adsorbed ethanol (**Figs. 8 and 9**) cannot be taken as a definite proof but only as an evidence that the observed surface species is a possible precursor of the products. To prove these surface species are true reaction intermediates, additional spectrokinetic methods need to be employed and which will be discussed in Section 5.4.^{7, 13-17, 23}

5.3.2. IFT phase domain results. It was shown in the previous section that spectra reconstruction is adequately performed via IDFT after filtering of signals that respond to the fundamental modulation frequency. Here, **Fig. 10** shows the in situ ME-PSD-DRIFTS phase domain spectra filtered at the fundamental modulation frequency ($1f_0 = 0.011$ Hz) over an entire period

cycle during ethanol conversion on γ - Al_2O_3 . While **Fig. 9B** shows a single spectrum at the maximum C–H stretching (2967 cm^{-1}) and at the frequency response of $1f_0$, **Fig. 10A** presents the phase domain contour plot which reflects spectra changes over one modulation period (90 s) as indicated in the Y axis. It is worth noting that, for simplicity, a sine waveform was added to this plot to guide the eye for gas phase concentration modulation, despite not being the actual modulation form. In general, this plot can be quite useful (if wavenumber and high and low absorbance ranges are selected appropriately) as it allows a quick visual evaluation of the possible presence of peaks and their possible relationships. In **Fig. 10A**, color contrast between blue and red regions correlate with low and high surface coverage of species with respect to a mid-point in the periodic modulation. More specifically, it can be quickly noticed that at high concentrations of ethanol in the gas feed (between ~25–60 s) there is an abundance of ethanol derived species as inferred from the C–H stretching at 3000 – 2800 cm^{-1} . These species seem to follow an opposite behavior to Al hydroxyl species in the 3800 – 3700 cm^{-1} region as shown by the blue color indicating a negative signal with respect to the average value during the periodic feed oscillation. Additionally, adsorbed water and ethanol bonded to hydroxyl groups were visible at high ethanol gas phase concentrations as indicated by the orange region between 3500 and 3100 cm^{-1} . The opposite observations can be also made when the concentration of ethanol is low (i.e., 60–90 s) because of the symmetry of the feed modulation and, therefore, the phase-domain spectra around a mid-concentration reference point. Such rapid evaluation of trends is only possible in this contour plot, which is not obvious from time domain spectra (**Fig. 7**).

More detailed observations can be made from individual in situ ME-PSD-DRIFTS phase domain traces shown in **Fig. 10B**. In contrast with the time domain plot (**Fig. 7**), the surface species observed in this plot respond to the fundamental feed concentration modulation and are possible reaction intermediates. This plot also shows that the PSD procedure significantly reduced the noise level and enhanced the definition of weak peaks, not easily discernible in the time domain spectra. At the reaction temperature investigated (473 K), the predominant product of reaction was diethyl ether followed by smaller amounts of ethylene. Therefore, from **Fig. 6** several surface species would be expected in the DRIFTS spectra such as adsorbed ethanol and ethoxide species. The following peaks were observed in **Fig. 10B**: 1) 2968, 2925, 2880, 1448, 1388, and very weak 1063 cm^{-1} , assigned to adsorbed ethanol;^{51, 86, 92-96} 2) 2968, 2925, 2880, 1448, 1388, and very weak (hardly distinguishable above noise level in a frequency domain magnitude plot, **Fig. S5**) 1137 , 1063 , and 1033 cm^{-1} , assigned to an incipient ethoxide species;^{51, 86, 92-96} 3) 3754, 3741, 3720, and 3680 cm^{-1} assigned to terminal and bridging hydroxyls in Al_IV and Al_V ;^{51, 87, 88, 97, 98} and 4) broad peak at 3500 – 3000 cm^{-1} assigned to ethanol and water H-bonded to surface hydroxyls in terminal and triply bridging positions on tetrahedral and octahedral Al .^{51, 87, 88, 97-99} These results are consistent with the conversion of ethanol to diethyl ether on γ - Al_2O_3 via an $\text{S}_\text{N}2$ mechanism involving an ethanol and an

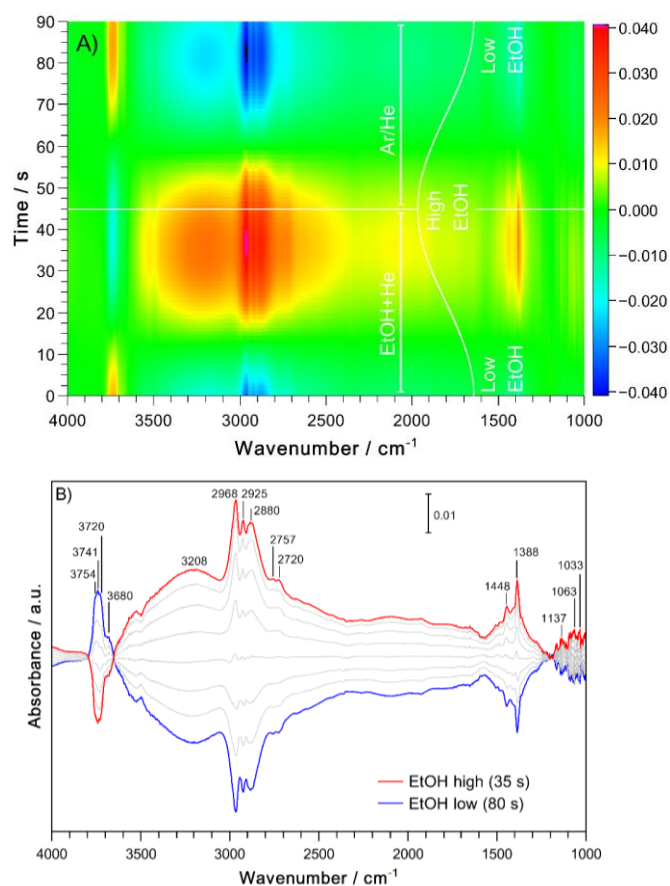


Fig. 10. In situ ME-PSD-DRIFTS spectra during ethanol conversion on γ - Al_2O_3 . A) Phase domain contour plot; B) Phase domain trace plot. Conditions: 473 K, 101.3 kPa, feed modulation from He/Ar \rightarrow He + EtOH (1 kPa), modulation frequency = $1/90$ Hz (period = 90 s), frequency response = $1/90$ Hz ($1f_0$), total gas flow ~ 45 NTP cm^3/min , catalyst weight ~ 45 mg. Phase angle = (time in s/period in s) $\times 360^\circ$. EtOH sine wave feed composition curve added to contour plot to guide the eye.

incipient ethoxide species (Fig. 6) in agreement with previous reports.^{82, 83, 86, 96, 100-103} Additionally, the results of Fig. 10B clearly show that several types of Al hydroxyl species, not just one, are likely active sites for ethanol conversion on γ -Al₂O₃. Also, the presence of the broad band at 3500–3000 cm⁻¹ indicates that ethanol and water molecules covered the catalyst surface to a large extent. As shown in Fig. 9C, some of these species respond much more slowly than other observed surface species. Such differences suggest the involvement of these species in the reaction mechanism, but not necessarily in the ethanol conversion catalytic cycle. This is in agreement with the involvement of these species as inhibitors during ethanol dehydration reactions as previously reported for ethanol, *n*-propanol, and isopropanol conversion on γ -Al₂O₃.^{83, 85, 90, 104}

5.3.3. IFT phase angle (argument) results. Another advantage of ME-PSD methodology is the possibility of discriminating surface species that have different kinetic responses in a catalytic or an adsorption/desorption cycle. This is seen as a phase lag in the response signal of the surface species with respect to the input signal waveform.^{10, 18, 24, 35} Such time or phase lag of surface species with different kinetic characteristics (i.e., time constant or relaxation time of reaction) resembles that observed in Figs. 4 and 5 (and Figs. S1-S2) as a result of different gas residence times in the in situ cell. Additionally, analysis of different peaks in a phase angle plot, that is, if they are in-sync (in-phase) or out-of-sync (out-of-phase) will provide information of the relationships of different species and thus of reaction pathways.^{10, 35, 37} A typical qualitative analysis of the kinetic response of different signals consists of comparing the relative response of the different species (e.g., peaks) at different times during a modulation period, as typically shown in: 1) a wavenumber vs absorbance phase domain plots with traces at different times (or phase angle)³⁵ (Fig. 10B) or 2) wavenumber vs phase angle plot (or phase shift or argument plot) at the frequency of interest (Fig. 11A).^{10, 37}

The phase domain plot (e.g., Fig. 10B) is quite useful because it only shows the signals of species that respond to input (e.g., feed concentration) modulation and which are possible intermediate species. When a phase domain spectrum presents species that are consumed and produced concomitantly, and which are interrelated, then both peaks will show opposite trends at different times (or phase angle) in a periodic cycle. Such kinetic differentiation should be then observed in a phase angle (argument) plot such as that shown in Fig. 11A. For example, this figure shows:

1) That all peaks in the 3600–1200 cm⁻¹ range are in-sync (in-phase) as they present the same phase angle. This suggests that these species have the same kinetic response (e.g., time constant) or that they all have fast kinetics (but not necessarily the same) so that they are able to follow the input modulation such as adsorbed ethanol or ethoxide species. Also, Fig. 9C indicated that some of the water and/or ethanol species H-bonded to surface hydroxyls in terminal and triply bridging positions on tetrahedral and octahedral Al adsorbed more slowly than others, but those that adsorb faster do so at similar rates as ethanol or

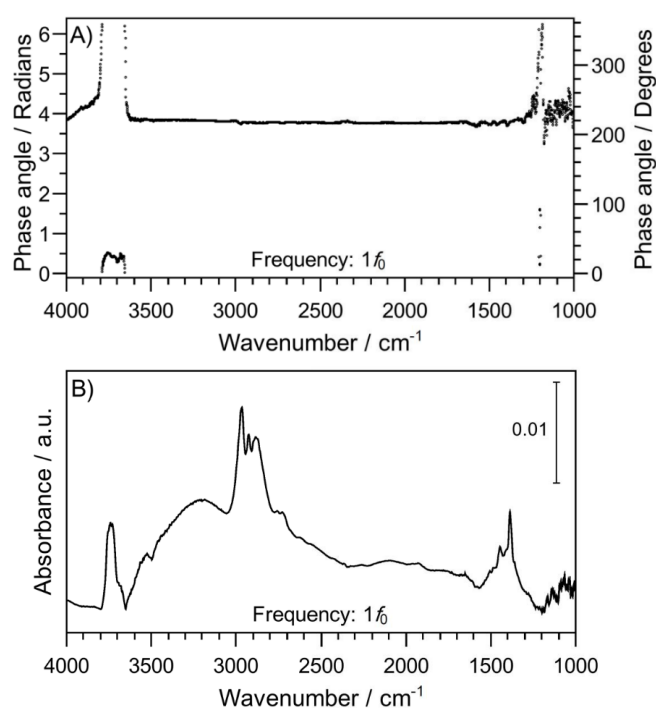


Fig. 11. In situ ME-PSD-DRIFTS during ethanol conversion on γ -Al₂O₃. A) phase angle (argument) plot at a frequency of 0.011 Hz; B) phase domain magnitude plot (showing all positive observed peaks) at a frequency of 0.011 Hz. Conditions: 473 K, 101.3 kPa, feed modulation from He/Ar \rightarrow He + EtOH (1 kPa), modulation frequency = 1/90 Hz, total gas flow \sim 45 NTP cm³/min, catalyst weight \sim 45 mg. Phase angle = (radians/2 π) \times 360°.

- ethoxide species on terminal and bridging hydroxyls in Al_{IV} and Al_V.
- That adsorbed ethanol or ethoxide species (3600–1200 cm⁻¹) are out-of-sync (out-of-phase) with respect to terminal and bridging hydroxyls in Al_{IV} and Al_V (3760–3650 cm⁻¹). This result suggests that ethanol/ethoxide species adsorb while hydroxyl species are consumed. This suggestion agrees with similar observations in the phase domain contour plot (Fig. 10A).
 - The different terminal and bridging hydroxyls in Al_{IV} and Al_V (3760–3650 cm⁻¹) kinetic response is similar, with the hydroxyls at 3720 cm⁻¹ (25.6°) showing a slightly larger kinetic response than 3755 cm⁻¹ (30.0°) \approx 3741 cm⁻¹ (27.8°) \approx 3680 cm⁻¹ (28.5°). These results suggest that at the studied conditions, terminal and bridging hydroxyls are likely reaction intermediates, but with the HO- μ_1 -Al_V (110) (@ 3720 cm⁻¹)^{87, 88, 97, 98} reacting at a slightly faster rate.
 - The noise level in the 1200–1000 cm⁻¹ is quite significant (Fig. S5) and no bands are discernible in the time domain. The noise is likely to arise from strong absorption of Al₂O₃, ambient photon, and/or reflection on the cell walls. In the phase domain, weak bands were observed with a slightly better signal-to-noise ratio (Fig. S5). While the magnitude of the fundamental modulation frequency is noticeable, it is only slightly above the noise level which precludes a conclusive assignment of the bands in this region.
 - The apparent significant phase lag observed around 1200 cm⁻¹ is an artifact calculated from noise as no peaks are observed in this region. To confirm or rule out the presence of peaks, a phase domain magnitude plot at the same

response frequency of 0.011 Hz such as that shown in Fig. 11B can be used. The figure serves as a guide to evaluate the observed peaks in the phase domain (Fig. 10B) as they all showed in the positive direction.

Gas phase ethanol contributions to the DRIFTS signal can be ruled out from comparison of Fig. 11B with the gas phase IR spectrum of ethanol (Fig. S6).

5.4. Limitations and future opportunities

One of the biggest challenges in in situ DRIFTS is the disentangling of intermediate species signals with those of spectators, background, and noise. ME-PSD-DRIFTS thus has become a powerful technique that allows to extract signals that possibly arise from intermediate species. Its application to the study of heterogeneous catalysts, however, have only been reported in the past 7 years from a handful of groups: Ferri and co-workers,^{36, 71, 74-77} Baiker and co-workers,^{39, 105, 106} Collins and co-workers,^{37, 78-80} and Hermans and co-workers^{38, 107} who used commercial (e.g., Harrick, Specac, Spectra-tech, Pike) and homemade in situ cells. With the exception of a homemade low-volume cell,^{39, 105, 106} it is very unlikely that any of the commercial DR cells possesses low void volumes < 1–2 cm³.^{2, 48, 49} As described in previous sections, low void-volume DR cells are more convenient for ME-PSD-DRIFTS studies because they allow the use of low residence times (<1–2 s) at reasonable gas flow rates (<100 cm³/min).⁴⁸

With regards to the in situ reaction cell design and operation, other aspects are worth to keep in mind for the ME-PSD-DRIFTS experiments (and any in situ experiment in general) which were recently reviewed.² These include, for example, 1) effective reactants-catalyst contact and well-mixed behaviour; 2) absence of transport limitations; 3) facile construction, low cost, and reproducibility; 4) well-defined residence time distribution; 5) isothermality; 6) operation conditions flexibility; 7) simple sampling, analysis of products, and operation and maintenance.^{108, 109} Several of these were reported for the low-void volume cell employed in the present work.⁴⁸ For example, it was shown that its design was simple and reproducible and easy to operate and maintain.⁴⁸ This in situ low-void volume cell could be fairly described as a well-mixed (CSTR) reactor allowing a good contact between feed gas and catalyst, and which also allowed the modelling and simulation presented in Section 4.4.1. The presence of a relatively low void volume permitted rapid exchange of gases within the cell, which is convenient for ME-PSD experiments (Section 4.4). Additionally, the cell could be integrated and was made compatible with commercial Harrick Scientific's mirror optics and accessories; it could fit in most commercial spectrometers and product sampling can be done via an online gas chromatograph or mass spectrometer. While no kinetics analysis was performed in the present work, care should be taken to ensure differential operation to facilitate analysis and avoid mass transfer limitations.

Another aspect that needs close attention is the measurement of sample temperature and the possible presence of temperature gradients within the sample. In the cell used in this work, the temperature was monitored by a

thermocouple that was in direct contact with the catalyst just below the sample top surface. This location ensured a measurement that was representative of the sample surface temperature where spectroscopic measurements took place. While temperature measurements remained constant during the ME experiments reported here, it is worth cautioning that within the small space of the sample volume there may be temperature gradients. This is an issue that is present in most in situ cells as a result of heat losses via radiation, conduction, and convection as reported for transmission and diffuse reflectance cells. For example, in the case of commercial cells^{49, 110, 111} and the low void volume cell,⁴⁸ temperature differences between the middle of the catalyst and the outer part of the cell could vary by as much as 20–120 °C, for sample bed temperatures as high as 500 °C. This is a worst-case scenario value because the gradients within the sample are expected to be smaller and are dependent on the reaction under study (e.g., exothermic vs endothermic), the sample bed temperature, and the carrier gas properties (e.g., heat capacity). Nevertheless, if significant, temperature gradients can corrupt kinetic measurements as previously reported.^{111, 112} In diffuse reflectance cells, such gradients can be minimized by reducing heat losses, for example, in the case of: 1) radiative, by changing the windows design or keeping the surrounding temperature high enough (without blocking the IR beam path or damaging the IR windows);¹⁰⁸ 2) convective, by employing ceramic materials to isolate the same cup or increasing the cooling liquid temperature; and 3) conductive, by preheating gases to the cell and employing carrier gases with relatively low heat capacity (e.g., Ar).^{48, 49}

There are two main reasons that have hindered further popularization of the ME-PSD-DRIFTS technique:¹⁸ 1) the lack of low void-volume commercial cells or reproducible homemade cells;^{2, 48} and 2) the apparent complexity of the numerical method required to implement the PSD methodology.^{6, 10, 24} Regarding 1), we have recently reported a low void-volume cell (including blueprints for reproduction in catalysis labs with machining capabilities);⁴⁸ and with respect to 2), we hope the current work can contribute to a better understanding of Fourier analysis for implementation of the PSD methodology. Unlike previous reports,^{6, 10, 24} the methodology described here is based on FFT and IFFT functions available in popular software packages (e.g., Matlab, Octave, Python) which can reduce the time for writing a homemade software while minimizing the chance for coding errors.

The methodology presented in this work not only introduced some general guidelines for planning and interpreting of ME-PSD-DRIFTS experiments, but also of possible new avenues for future research. For example, frequency domain plots have not been exploited despite carrying information on the background, spectator species, baseline shifts (e.g., due to accumulation of nonreactive species), time-dependent amplitude changes, and response frequencies of intermediate species. Therefore, new information of surface species could be afforded from careful choice of ME and reaction conditions and analysis of frequency features in, for example, a frequency domain magnitude plot.

Two examples of future development were put forward: 1) the use of a decaying input modulation waveform to obtain rapid kinetic information of surface species (Section 4.2) in a single experiment, rather than with several experiments of varying input modulation frequencies; and 2) the study of kinetics of rapidly deactivating catalysts by analysis of the broadening of frequency signals analogous to NMR relaxation techniques in the frequency domain. Since ME-PSD has only been applied to stable catalysts, ME-PSD-DRIFTS can provide new understanding on the active sites and surface species involved during the deactivation of catalysts.

As described above, ME-PSD enhances spectra signal-to-noise ratio and allows the discrimination of species that respond to a periodic perturbation from those that do not (e.g., spectators). The phase domain IR spectra, however, are still affected by common issues found in IR such as the presence of multiple and overlapping peaks. While, temporal changes in the phase domain or analysis of phase angle shifts in argument plots assist in the determination of species with different kinetic response, this can become more difficult, for example, for complex chemistries with multiple surface species. One alternative approach that can complement ME or ME-PSD is 2D correlation spectroscopy (2D COS) which can be applied to in situ spectra collected from catalysts exposed to non-periodic or periodic perturbations.⁶⁷ 2D COS can therefore be applied to ME time domain or ME-PSD phase domain data to help differentiate overlapped peaks via correlation of bands, enhance spectral resolution by use of the second dimension, and probe the order of changes in the observed peaks.¹¹³ Briefly, 2D COS, as developed by Noda,¹¹⁴⁻¹¹⁶ plots spectral intensity against two independent spectra variables (e.g., in the case of 2D COS IR they could be wavenumbers ν_1 and ν_2) to quantitatively compare their intensity variations. From a ME experiment, the collected IR spectra can be also manipulated mathematically to yield 2D correlation plots between the independent variables. 2D COS, just like PSD, uses Fourier analysis to define a correlation intensity equation; however, in the case of ν_1 and ν_2 2D COS, it does so by combining the FT of intensity variations of ν_1 with the FT conjugate of ν_2 . Such correlation can be expressed as a complex number comprising two orthogonal components which define the 2D spectral plots for COS analysis: the *synchronous* (real part) and *asynchronous* (imaginary part) components. Such 2D plots enable the correlation of bands that are in- or out-of-phase and the determination of order at which they change intensities, respectively, facilitating the discrimination of complex overlapped bands and their response kinetics.¹¹⁶ The literature on 2D COS applied to characterization of heterogeneous catalysts is rather scarce. However, examples of its application to non-periodic perturbation of catalytic materials as followed by in situ IR have been reported.¹¹⁷⁻¹²⁰

As in situ/operando spectroscopic studies become more routine, there is a need to move from qualitative to quantitative studies. This is no easy task because of the difficulties in the calibration of spectroscopic signals. Some examples can be found in the literature for the determination of reaction rates of surface species¹⁵ and in particular when combined with

steady state isotopic transient kinetic analysis (SSITKA) technique.^{13, 14} Such techniques could be also applied to the reconstructed spectra after the PSD methodology to gain information on individual surface species kinetics. Moreover, the combination of SSITKA with ME-PSD-DRIFTS has been demonstrated and will undoubtedly represent a powerful combination to explore reaction intermediate species and their kinetics.^{38, 105, 106} This unconventional SSITKA at periodic ME conditions also provides additional information to discriminate and identify surface species and their dynamics. However, no quantitative analysis of residence time, concentration, or reaction rates of adsorbed species has been reported for SSITKA-ME-PSD-DRIFTS as it has been done in SSITKA-DRIFTS experiments.^{19, 20, 121} In conventional SSITKA, kinetic isotope effect (KIE) measurements are also possible at the start and end of a run where a single unlabelled or isotopically labelled reactant is present.^{14, 122} However, this is not feasible in a SSITKA-ME-PSD where mixed isotopologues are present at all periodic conditions. Future developments of a mathematical framework to account for periodic changes of surface species should help quantify reaction intermediates and KIE in SSITKA-ME-PSD-DRIFTS experiments.

In this natural evolution from in situ to operando and from spectroscopic to spectrokinetic studies, careful consideration should be given to the reaction cell and reaction conditions.^{2, 13, 109} As discussed above, low void-volume DR cells and proper choice of modulation frequency and amplitude change can help simplify ME kinetic models to obtain information on rate constants of individual elementary steps. For such a purpose, the early works by Renken,²⁸ Wokaun,³¹⁻³⁴ and Gonzalez²⁷ provide examples of kinetic studies from in situ ME-DRIFTS experiments which could be further extended to ME-PSD-DRIFTS. Kinetic studies in transient conditions^{61, 65} and in combination with kinetic models that consider surface species¹²³⁻¹²⁵ can also serve as inspiration for further quantitative developments of ME-PSD-DRIFTS.

Lastly, in the application of ME-PSD-DRIFTS technique, it should be noted that while the species detected by ME-PSD respond to feed modulation, this alone does not indicate that these species are true reaction intermediates. Such observation was first made by Tamaru more than 50 years ago, which set the stage for the development of transient spectrokinetic techniques.¹²⁶ Tamaru was also the first to propose and develop dynamic techniques to demonstrate the identity of a true surface intermediate species by in situ IR via a "stopped-reactant" type method¹²⁶⁻¹³¹ and of reversibly adsorbed species by an isotopic jump method^{132, 133} which resembles the SSITKA technique. The former dynamic technique consists of: 1) recording simultaneous or parallel spectroscopic and fixed-bed reactor kinetic measurements; 2) determining quantitatively the adsorbed species kinetic response, for example, by independent determination (i.e., calibration) of surface coverages; and 3) comparing reaction rates calculated from surface coverages (e.g., via spectroscopy) with that measured in the experiment (e.g., via MS or GC). A close matching (e.g., same order of magnitude) of both reaction rates proves the species is a true surface reaction intermediate. More recent

developments of the method have been reported by Oyama and co-workers^{15-17, 134} and Meunier and co-workers.^{13, 135, 136}

While in situ and operando spectroscopic characterization of heterogeneous catalysts is far from perfect, complementary spectrokinetic techniques remain at present one of our best tools for assessment of true surface reaction intermediates. This also applies to modern ME-PSD dynamic methods, which in absence of additional or control spectrokinetic studies, are unable to discriminate true intermediate or reversibly adsorbed surface species. It could be argued that ME-PSD-DRIFTS does not generate more information than the traditional stop-reactant type methods. For example, time domain response of medium to large size peaks observed in the phase domain also evidences a visible response to the gas phase perturbation (Figs. S3-S5). However, it is clear from this contribution that ME-PSD-DRIFTS offers significant advantages that enhance the analysis of detected surface species including: 1) collection and averaging of a large number of experiments over a relatively short period of time which reduces the noise level while enhancing signal and definition of peaks (in the phase domain) that may not be easily discernible in the time domain; 2) rapid evaluation for the presence of peaks and possible relationship among them and dynamic response via frequency domain and contour, trace view, argument, and magnitude plots of the phase domain. Clearly, Tamaru's spectrokinetic approach could be also adapted for future developments of ME-PSD-DRIFTS and SSITKA-ME-PSD-DRIFTS. Additionally, application of ME-DRIFTS simple microkinetic models, as reported by Gonzalez,²⁷ Renken,²⁸ and Wokaun,³¹⁻³⁴ for the determination of rate constants of adsorption and of elementary steps (even in the absence of calibration) could be further extended to ME-PSD-DRIFTS for discrimination of intermediate species via kinetic analysis of phase shifts at varying modulation frequencies.^{26, 137, 138}

To summarize, despite the limitations of ME-PSD-DRIFTS, there are many opportunities to further advance the technique, including, for example, by combination with SSITKA, 2D COS, and transient spectrokinetics via conventional stop reactant methods and microkinetic analysis. Such developments will without a doubt assist in the discrimination of true surface reaction intermediates and further our understanding of heterogeneously catalyzed reactions.

6. Conclusions

In this work, the application of modulation excitation-phase sensitive detection-diffuse reflectance Fourier transform spectroscopy (ME-PSD-DRIFTS) via discrete Fourier transform (DFT)/inverse discrete Fourier transform (IDFT) was described in detail including a general mathematical framework, basic guidelines for planning, running, and interpreting ME-PSD-DRIFTS results with aspects such as required modulation frequency and amplitude, modulation waveform, sampling rate, and in situ cell residence time. The described ME-PSD technique was based on the introduction of a periodic perturbation in the reaction system so that PSD can be applied via Fourier analysis. For this analysis, the resulting spectroscopic

data was converted from time domain to frequency domain via DFT, followed by selection of a proper response frequency (or frequencies), and reconstruction of the filtered signal via IDFT. Because spectator species do not respond to rapid modulation frequencies in the range of reaction turnover frequencies, the methodology allows the sensitive detection of reacting species that respond to the modulation frequency, which are, thus, possible reaction intermediates. The resulting filtered spectra in the so-called phase domain and phase angle (i.e., argument) plots permitted the study of the relative response of the various detected species. Additionally, the use of frequency domain plots provided information on the reaction system such as baseline shifts (e.g., due to accumulation of spectator species on the catalyst surface), signal response to modulation, response waveform type, noise, and signal decay/growth, which have not been explored in previous applications of ME-PSD. Because the described DFT/IDFT procedure can be applied to any periodic modulation, in theory, any input modulation waveform (not just sine and square waveforms) can be used to introduce a perturbation in the reaction system. In practice, this is quite convenient as a single software code can be used to handle ME-PSD responses regardless of the type of periodic perturbation. Future applications were discussed including the kinetic study from decaying/growing input signals of surface reacting species on stable or deactivating catalysts. Because of the general application of the ME-PSD methodology, we also expect this work to promote its popularization and application not only to DRIFTS but also to IR in general and other in situ/operando spectroscopic techniques and thus contribute to the further understanding of active sites and intermediate species in heterogeneous catalysis.

7. Conflicts of interest

There are no conflicts to declare.

8. Acknowledgements

Acknowledgment is made to the Donors of the American Chemical Society Petroleum Research Fund for support of this research, grant No 58044-DNI5. The authors also acknowledge financial support by the National Science Foundation, grant No OIA-1539105. We also dedicate this manuscript to Professor Kenzi Tamaru. His pioneering work on in situ and operando characterization of catalysts and evaluation of surface reaction intermediates has served as a true inspiration for catalysis researchers. His ideas and work motivated the present research to advance in situ spectroscopic tools for the catalysis community that facilitate the detection of surface species. As stressed by Professor Tamaru, we also hope these tools can help determine adsorbed species as true reaction intermediates in heterogeneously catalyzed reactions.

9. References

- 1 J.J. Bravo-Suárez, R.V. Chaudhari, B. Subramaniam, Design of Heterogeneous Catalysts for Fuels and Chemicals Processing: An Overview, in: *Novel Materials for Catalysis and Fuels Processing*, J.J. Bravo-Suárez, M.K. Kidder, V. Schwartz, Eds., American Chemical Society, Washington, D.C., 2013, pp. 3-68.
- 2 J.J. Bravo-Suárez, P.D. Srinivasan, *Catal. Rev.- Sci. Eng.*, 2017, pp1-151, <https://doi.org/10.1080/01614940.01612017.01360071>.
- 3 In: *In-Situ Spectroscopy of Catalysts*, Ed., B.M. Weckhuysen, American Scientific Publishers, Stevenson Ranch, CA, 2004, pp. 1-332
- 4 M. Che, J.C. Vedrine, Characterization of Solid Materials and Heterogeneous Catalysts: From Structure to Surface Reactivity, Wiley, Weinheim, Germany, 2012, pp. 1-1181.
- 5 C. Lamberti, A. Zecchina, E. Groppo, S. Bordiga, *Chem. Soc. Rev.*, 2010, **39**, 4951-5001.
- 6 D. Baurecht, U.P. Fringeli, *Rev. Sci. Instrum.*, 2001, **72**, 3782-3792.
- 7 F.C. Meunier, *Chem. Soc. Rev.*, 2010, **39**, 4602-4614.
- 8 B.M. Weckhuysen, *Phys. Chem. Chem. Phys.*, 2003, **5**, 4351-4360.
- 9 V. Marchionni, D. Ferri, O. Krocher, A. Wokaun, *Anal. Chem.*, 2017, **89**, 5802-5810.
- 10 A. Urakawa, T. Bürgi, A. Baiker, *Chem. Eng. Sci.*, 2008, **63**, 4902-4909.
- 11 J. Pérez-Ramírez, E.V. Kondratenko, *Catal. Today*, 2007, **121**, 160-169.
- 12 K. Morgan, N. Maguire, R. Fushimi, J.T. Gleaves, A. Goguet, M.P. Harold, E.V. Kondratenko, U. Menon, Y. Schuurman, G.S. Yablonsky, *Catal. Sci. Technol.*, 2017, **7**, 2416-2439.
- 13 F.C. Meunier, *Catal. Today*, 2010, **155**, 164-171.
- 14 C.M. Kalamaras, S. Americanou, A.M. Efstathiou, *J. Catal.*, 2011, **279**, 287-300.
- 15 J.J. Bravo-Suárez, K.K. Bando, J.I. Lu, M. Haruta, T. Fujitani, S.T. Oyama, *J. Phys. Chem. C*, 2008, **112**, 1115-1123.
- 16 S.T. Oyama, W. Li, *Top. Catal.*, 1999, **8**, 75-80.
- 17 T. Gott, S.T. Oyama, *J. Catal.*, 2009, **263**, 359-371.
- 18 P. Müller, I. Hermans, *Ind. Eng. Chem. Res.*, 2017, **56**, 1123-1136.
- 19 S.L. Shannon, J.G. Goodwin, *Chem. Rev. (Washington, DC, U.S.)*, 1995, **95**, 677-695.
- 20 C. Ledesma, J. Yang, D. Chen, A. Holmen, *ACS Catal.*, 2014, **4**, 4527-4547.
- 21 S.S.C. Chuang, F. Guzman, *Top. Catal.*, 2009, **52**, 1448-1458.
- 22 In: *In-Situ Characterization of Heterogeneous Catalysts*, Eds. J.A. Rodriguez, J.C. Hanson, P.J. Chupas, Wiley, Hoboken, NJ, 2013, pp. 1-488
- 23 R. Kopelent, J.A. van Bokhoven, J. Szlachetko, J. Edebeli, C. Paun, M. Nachttegaal, O.V. Safonova, *Angew. Chem., Int. Ed.*, 2015, **54**, 8728-8731.
- 24 A. Urakawa, T. Bürgi, A. Baiker, *Chem. Phys.*, 2006, **324**, 653-658.
- 25 L. Polinski, L. Naphtali, *Adv. Catal.*, 1969, **19**, 241-291.
- 26 R.H. Jones, D.R. Olander, W.J. Siekhaus, J.A. Schwarz, *J. Vac. Sci. Technol.*, 1972, **9**, 1429-1441.
- 27 Y.-E. Li, D. Willcox, R.D. Gonzalez, *AIChE J.*, 1989, **35**, 423-428.
- 28 M. Marwood, R. Doepper, A. Renken, *Can. J. Chem. Eng.*, 1996, **74**, 660-663.
- 29 M. Cavers, J.M. Davidson, I.R. Harkness, L.V.C. Rees, G.S. McDougall, *J. Catal.*, 1999, **188**, 426-430.
- 30 M. Cavers, J.M. Davidson, I.R. Harkness, G.S. McDougall, L.V.C. Rees, *Stud. Surf. Sci. Catal.*, 1999, **122**, 65-72.
- 31 E.E. Ortelli, J. Wambach, A. Wokaun, *Appl. Catal., A*, 2000, **192**, 137-152.
- 32 E.E. Ortelli, A. Wokaun, *Vib. Spectrosc.*, 1999, **19**, 451-459.
- 33 J. Kritzenberger, A. Wokaun, *J. Mol. Catal. A: Chem.*, 1997, **118**, 235-245.
- 34 E.E. Ortelli, J. Wambach, A. Wokaun, *Appl. Catal., A*, 2001, **216**, 227-241.
- 35 T. Bürgi, A. Baiker, *J. Phys. Chem. B*, 2002, **106**, 10649-10658.
- 36 R. Kydd, D. Ferri, P. Hug, J. Scott, W.Y. Teoh, R. Amal, *J. Catal.*, 2011, **277**, 64-71.
- 37 A. Aguirre, S.E. Collins, *Catal. Today*, 2013, **205**, 34-40.
- 38 P. Müller, S.P. Burt, A.M. Love, W.P. McDermott, P. Wolf, I. Hermans, *ACS Catal.*, 2016, **6**, 6823-6832.
- 39 N. Maeda, F. Meemken, K. Hungerbühler, A. Baiker, *Chimia*, 2012, **66**, 664-667.
- 40 A. Urakawa, W. Van Beek, M. Monrabal-Capilla, J.R. Galán-Mascarós, L. Palin, M. Milanesio, *J. Phys. Chem. C*, 2011, **115**, 1323-1329.
- 41 D. Ferri, M.A. Newton, M. Nachttegaal, *Top. Catal.*, 2011, **54**, 1070-1078.
- 42 D. Ferri, M.A. Newton, M. Di Michiel, G.L. Chiarello, S. Yoon, Y. Lu, J. Andrieux, *Angew. Chem., Int. Ed.*, 2014, **53**, 8890-8894.
- 43 In: *Transform Techniques in Chemistry*, Ed., P.R. Griffiths, Plenum Press, New York, NY, 1978, pp. 1-385
- 44 E.O. Brigham, *The Fast Fourier Transform and Its Applications*, Prentice Hall, Englewood Cliffs, NJ, 1988, pp. 1-448.
- 45 J. Kauppinen, J. Partanen, *Fourier Transforms in Spectroscopy*, Wiley, Berlin, Germany, 2001, pp. 1-271.
- 46 T.M. Peters, J.C. Williams, *The Fourier Transform in Biomedical Engineering*, Birkhäuser Boston, New York, NY, 1998, pp. 1-199.
- 47 FFTW. <http://www.fftw.org/> (Accessed: Dec. 16, 2018).
- 48 B.S. Patil, P.D. Srinivasan, E. Atchison, H. Zhu, J.J. Bravo-Suárez, *React. Eng. Chem.*, 2018, (DOI: 10.1039/c1038re00302e).
- 49 P.D. Srinivasan, S.R. Nitz, K.J. Stephens, E. Atchison, J.J. Bravo-Suárez, *Appl. Catal., A*, 2018, **561**, 7-18.
- 50 J. Sirta, S. Phanichphant, F.C. Meunier, *Anal. Chem.*, 2007, **79**, 3912-3918.
- 51 P.D. Srinivasan, K. Khivantsev, J.M.M. Tengco, H. Zhu, J.J. Bravo-Suárez, *Submitted*, 2018.
- 52 M.L. Meade, *Lock-in Amplifiers: Principles and Applications*, P. Peregrinus, London, UK, 1983, pp. 1-232.
- 53 J.A. Dávila Pintle, *Rev. Mex. Fis. E*, 2013, **59**, 1-7.
- 54 In: *Composition Modulation of Catalytic Reactors (Topics in Chemical Engineering, Vol. 11)*, Ed., P.L. Silvertown, Gordon and Breach Science Publishers, Amsterdam (The Netherlands), 1998, pp. 1-596
- 55 S.C. Reyes, E. Iglesia, Frequency Response Techniques for the Characterization of Porous Catalytic Solids, in: *Catalysis*, J.J. Spivey, S.K. Agarwal, Eds., The Royal Society of Chemistry, 1994, pp. 51-92.
- 56 K.T. Tang, *Mathematical Methods for Engineers and Scientists 3: Fourier Analysis, Partial Differential Equations and Variational Methods*, Springer, Berlin, Germany, 2007, pp. 1-440.
- 57 J.C. Santamarina, D. Fratta, *Discrete Signals and Inverse Problems: An Introduction for Engineers and Scientists*, Wiley, Chichester, UK, 2005, pp. 1-364.
- 58 J.F. James, *A Student's Guide to Fourier Transforms: With Applications in Physics and Engineering*, 3rd ed., Cambridge University Press, Cambridge, UK, 2011, pp. 1-146.
- 59 R.G. Lyons, *Understanding Digital Signal Processing*, Prentice Hall, Upper Saddle River, NJ, 2004, pp. 1-665.

- 60 P. Silveston, R.R. Hudgins, A. Renken, *Catal. Today*, 1995, **25**, 91-112.
- 61 C.F. Bernasconi, *Relaxation Kinetics*, Academic Press, London, U.K, 1976, pp. 1-288.
- 62 In: *Catalysis under Transient Conditions*, ACS Symposium Series, 178, Eds. A.T. Bell, L.L. Hegedus, American Chemical Society, Washington, D.C., 1982, pp. 1-308
- 63 K. Tamaru, *Dynamic Relaxation Methods in Heterogeneous Catalysis*, in: *Catalysis: Science and Technology*, J.R. Anderson, M. Boudart, Eds., Springer, Berlin, Germany, 2012, pp. 87-129.
- 64 E.F. Caldin, *The Study of Fast Reactions in Solution*, in: *Techniques and Applications of Fast Reactions in Solution (Nato Advanced Study Institutes Series (Series C — Mathematical and Physical Sciences))*, W.J. Gettins, E. Wyn-Jones, Eds., Springer, Dordrecht, Holland, 1979, pp. 1-11.
- 65 M. Eigen, L. De Maeyer, *Tech. Org. Chem.*, 1963, **8**, 895-1054.
- 66 T. Bürgi, A. Baiker, *Adv. Catal.*, 2006, **50**, 227-283.
- 67 M. Muller, R. Buchet, U.P. Fringeli, *J. Phys. Chem.*, 1996, **100**, 10810-10825.
- 68 F.H. Ribeiro, A.E. Schach von Wittenau, C.H. Bartholomew, G.A. Somorjai, *Catal. Rev. - Sci. Eng.*, 1997, **39**, 49-76.
- 69 S.W. Smith, *The Scientist and Engineer's Guide to Digital Signal Processing*, 2nd ed., California Technical Publishing, San Diego, CA, 1997, pp. 1-650.
- 70 B. Li, R.D. Gonzalez, *Appl. Spectrosc.*, 1998, **52**, 1488-1491.
- 71 G.L. Chiarello, M. Nachtegaal, V. Marchionni, L. Quaroni, D. Ferri, *Rev. Sci. Instrum.*, 2014, **85**, 074102.
- 72 M.M. Schubert, T.P. Häring, G. Bräth, H.A. Gasteiger, R.J. Behm, *Appl. Spectrosc.*, 2001, **55**, 1537-1543.
- 73 V. Dal Santo, C. Dossi, A. Fusi, R. Psaro, C. Mondelli, S. Recchia, *Talanta*, 2005, **66**, 674-682.
- 74 V. Marchionni, M.A. Newton, A. Kambolis, S.K. Matam, A. Weidenkaff, D. Ferri, *Catal. Today*, 2014, **229**, 80-87.
- 75 J. Zarfl, D. Ferri, T.J. Schildhauer, J. Wambach, A. Wokaun, *Appl. Catal., A*, 2015, **495**, 104-114.
- 76 A. Haghofer, D. Ferri, K. Föttinger, G. Rupprechter, *ACS Catal.*, 2012, **2**, 2305-2315.
- 77 O. Martin, C. Mondelli, A. Cervellino, D. Ferri, D. Curulla-Ferre, J. Perez-Ramirez, *Angew. Chem., Int. Ed.*, 2016, **55**, 11031-11036.
- 78 A. Aguirre, C.E. Barrios, A. Aguilar-Tapia, R. Zanella, M.A. Baltanas, S.E. Collins, *Top. Catal.*, 2016, **59**, 347-356.
- 79 J. Vecchiotti, A. Bonivardi, W.Q. Xu, D. Stacchiola, J.J. Delgado, M. Calatayud, S.E. Collins, *ACS Catal.*, 2014, **4**, 2088-2096.
- 80 E. del Rio, S.E. Collins, A. Aguirre, X.W. Chen, J.J. Delgado, J.J. Calvino, S. Bernal, *J. Catal.*, 2014, **316**, 210-218.
- 81 T.E. Marlin, T. Marlin, *Process Control: Designing Processes and Control Systems for Dynamic Performance*, 2nd ed., McGraw-Hill, New York, NY, 2000, pp. 1-1017.
- 82 J.I. Di Cosimo, V.K. Díez, M. Xu, E. Iglesia, C.R. Apesteguía, *J. Catal.*, 1998, **178**, 499-510.
- 83 J.F. DeWilde, H. Chiang, D.A. Hickman, C.R. Ho, A. Bhan, *ACS Catal.*, 2013, **3**, 798-807.
- 84 K. Larmier, C. Chizallet, N. Cadran, S. Maury, J. Abboud, A.-F. Lamic-Humblot, E. Marceau, H. Lauron-Pernot, *ACS Catal.*, 2015, **5**, 4423-4437.
- 85 K. Larmier, A. Nicolle, C. Chizallet, N. Cadran, S. Maury, A.-F. Lamic-Humblot, E. Marceau, H. Lauron-Pernot, *ACS Catal.*, 2016, **6**, 1905-1920.
- 86 T.K. Phung, A. Lagazzo, M.A.R. Crespo, V.S. Escribano, G. Busca, *J. Catal.*, 2014, **311**, 102-113.
- 87 G. Busca, *Adv. Catal.*, 2014, **57**, 319-404.
- 88 G. Busca, *Catal. Today*, 2014, **226**, 2-13.
- 89 J. Lee, E.J. Jang, H.Y. Jeong, J.H. Kwak, *Appl. Catal., A*, 2018, **556**, 121-128.
- 90 J. Lee, J. Szanyi, J.H. Kwak, *Mol. Catal.*, 2017, **434**, 39-48.
- 91 J. Lee, E.J. Jang, J.H. Kwak, *J. Catal.*, 2017, **345**, 135-148.
- 92 P.Y. Sheng, G.A. Bowmaker, H. Idriss, *Appl. Catal., A*, 2004, **261**, 171-181.
- 93 M.A. Natal-Santiago, J.A. Dumesic, *J. Catal.*, 1998, **175**, 252-268.
- 94 K. Hemelsoet, A. Ghysels, D. Mores, K. De Wispelaere, V. Van Speybroeck, B.M. Weckhuysen, M. Waroquier, *Catal. Today*, 2011, **177**, 12-24.
- 95 J. Gao, A.V. Teplyakov, *J. Catal.*, 2013, **300**, 163-173.
- 96 T.K. Phung, G. Busca, *Chem. Eng. J. (Lausanne)*, 2015, **272**, 92-101.
- 97 K. Hadjiivanov, *Adv. Catal.*, 2014, **57**, 99-318.
- 98 M. Digne, P. Sautet, P. Raybaud, P. Euzen, H. Toulhoat, *J. Catal.*, 2002, **211**, 1-5.
- 99 K. Alexopoulos, M.-S. Lee, Y. Liu, Y. Zhi, Y. Liu, M.-F. Reyniers, G.B. Marin, V.-A. Glezakou, R. Rousseau, J.A. Lercher, *J. Phys. Chem. C*, 2016, **120**, 7172-7182.
- 100 M. Kang, A. Bhan, *Catal. Sci. Technol.*, 2016, **6**, 6667-6678.
- 101 S. Roy, G. Mpourmpakis, D.-Y. Hong, D.G. Vlachos, A. Bhan, R.J. Gorte, *ACS Catal.*, 2012, **2**, 1846-1853.
- 102 M.A. Christiansen, G. Mpourmpakis, D.G. Vlachos, *ACS Catal.*, 2013, **3**, 1965-1975.
- 103 Z. Fang, Y. Wang, D.A. Dixon, *J. Phys. Chem. C*, 2015, **119**, 23413-23421.
- 104 M. Kang, J.F. DeWilde, A. Bhan, *ACS Catal.*, 2015, **5**, 602-612.
- 105 M. Nobutaka, M. Fabian, B. Alfons, *ChemCatChem*, 2013, **5**, 2199-2202.
- 106 N. Maeda, F. Meemken, K. Hungerbühler, A. Baiker, *ACS Catal.*, 2013, **3**, 219-223.
- 107 P. Müller, S.-C. Wang, S.P. Burt, I. Hermans, *ChemCatChem*, 2017, **9**, 3572-3582.
- 108 F.C. Meunier, *React. Chem. Eng.*, 2016, **1**, 134-141.
- 109 N.E. Tsakoumis, A.P.E. York, D. Chen, M. Ronning, *Catal. Sci. Technol.*, 2015, **5**, 4859-4883.
- 110 J.J. Venter, M.A. Vannice, *Appl. Spectrosc.*, 1988, **42**, 1096-1103.
- 111 H. Li, M. Rivallan, F. Thibault-Starzyk, A. Travert, F.C. Meunier, *Phys. Chem. Chem. Phys.*, 2013, **15**, 7321-7327.
- 112 M.J. Wulfers, G. Tzolova-Müller, J.I. Villegas, D.Y. Murzin, F.C. Jentoft, *J. Catal.*, 2012, **296**, 132-142.
- 113 I. Noda, Y. Ozaki, *Two-Dimensional Correlation Spectroscopy: Applications in Vibrational and Optical Spectroscopy*, Wiley, Chichester, 2004, pp. 1-310.
- 114 I. Noda, *Appl. Spectrosc.*, 1990, **44**, 550-561.
- 115 I. Noda, *Appl. Spectrosc.*, 1993, **47**, 1329-1336.
- 116 I. Noda, A.E. Dowrey, C. Marcott, G.M. Story, Y. Ozaki, *Appl. Spectrosc.*, 2000, **54**, 236A-248A.
- 117 F. Thibault-Starzyk, A. Vimont, J.P. Gilson, *Catal. Today*, 2001, **70**, 227-241.
- 118 K.A. Tarach, K. Golabek, M. Choi, K. Gora-Marek, *Catal. Today*, 2017, **283**, 158-171.
- 119 D.K. Chlebda, P.J. Jodlowski, R.J. Jedrzejczyk, J. Lojewska, *Spectrochimica Acta Part a-Molecular and Biomolecular Spectroscopy*, 2018, **192**, 202-210.
- 120 K. Golabek, K.A. Tarach, K. Gora-Marek, *Microporous Mesoporous Mater.*, 2018, **266**, 90-101.
- 121 S. Pansare, A. Sirijaruphan, J. James G Goodwin Investigation of Reaction at the Site Level Using Ssitka, in: *Isotopes in Heterogeneous Catalysis*, pp. 183-211.

- 122 K. Polychronopoulou, A.M. Efstathiou, *Catal. Today*, 2006, **116**, 341-347.
- 123 B.J. Savatsky, A.T. Bell, Nitric Oxide Reduction by Hydrogen over Rhodium Using Transient Response Techniques, in: *Catalysis under Transient Conditions*, A.T. Bell, L.L. Hegedus, Eds., American Chemical Society, Washington, D.C., 1982, pp. 105-141.
- 124 C.G. Visconti, L. Lietti, F. Manenti, M. Daturi, M. Corbetta, S. Pierucci, P. Forzatti, *Top. Catal.*, 2013, **56**, 311-316.
- 125 S. Thomas, O. Marie, P. Bazin, L. Lietti, C.G. Visconti, M. Corbetta, F. Manenti, M. Daturi, *Catal. Today*, 2017, **283**, 176-184.
- 126 K. Tamaru, *Adv. Catal.*, 1965, **15**, 65-90.
- 127 K. Tamaru, *Bull. Chem. Soc. Jpn.*, 1958, **31**, 666-667.
- 128 K. Tamaru, *Nippon Kagaku Zasshi*, 1966, **87**, 1007-1013.
- 129 Y. Noto, K. Fukuda, T. Onishi, K. Tamaru, *Trans. Faraday Soc.*, 1967, **63**, 3081-3087.
- 130 K. Fukuda, Y. Noto, T. Onishi, K. Tamaru, *Trans. Faraday Soc.*, 1967, **63**, 3072-3080.
- 131 A. Ueno, T. Onishi, K. Tamaru, *Trans. Faraday Soc.*, 1970, **66**, 756-763.
- 132 K. Tamaru, *Proc. Jpn. Acad. Ser. B-Phys. Biol. Sci.*, 2004, **80**, 119-127.
- 133 K. Tamaru, *Dynamic Heterogeneous Catalysis*, Academic Press, New York, NY, 1978, pp. 1-140.
- 134 S.T. Oyama, W. Zhang, *J. Am. Chem. Soc.*, 1996, **118**, 7173-7177.
- 135 D. Lorito, A. Paredes-Nunez, C. Mirodatos, Y. Schuurman, F.C. Meunier, *Catal. Today*, 2016, **259**, 192-196.
- 136 A. Paredes-Nunez, D. Lorito, L. Burel, D. Motta-Meira, G. Agostini, N. Guilhaume, Y. Schuurman, F. Meunier, *Angew. Chem., Int. Ed.*, 2018, **57**, 547-550.
- 137 J.A. Schwarz, R.J. Madix, *J. Catal.*, 1968, **12**, 140-144.
- 138 J.A. Schwarz, R.J. Madix, *Surf. Sci.*, 1974, **46**, 317-341.

Application of modulation excitation-phase sensitive detection-DRIFTS for in situ/operando characterization of heterogeneous catalysts

Priya D. Srinivasan, Bhagyasha S. Patil, Hongda Zhu, and Juan J. Bravo-Suárez

A new more general method and guidelines for implementation of modulation excitation-phase sensitive detection-diffuse reflectance Fourier transform spectroscopy (ME-PSD-DRIFTS)

